

2018



**25th Congress of
International Federation for
Heat Treatment and Surface Engineering**

11-14 September 2018 | Xi'an China

PROCEEDINGS



Organized by Chinese Heat Treatment Society (CHTS)

25th IFHTSE CONGRESS PROCEEDINGS

11-14 September 2018

Xi'an China



Chinese Heat Treatment Society

Tel: +86 (0) 10 6292 0613 • Email: chts@chts.org.cn • Web: www.chts.org.cn

Add: 18 Xueqing Rd., Beijing, China

ID chromizing in power industry.....	228
High temperature oxidation performance of thick Cr coating using large arc deposition system for accident tolerant fuel claddings.....	229
Effect of precipitation hardening on the tensile behavior of a fccbased high-entropy alloy.....	229
High temperature oxidation behavior of molybdenum alloy thinwall tubes coated with FeCrAl.....	230
Study on microstructures and properties of high thermal conductivity tungsten-based materials prepared by spark plasma sintering.....	230
Corrosion inhibition performance of phenylaminomethylbenzotriazole in 5% HCl solution.....	231
Microstructure and transient laser thermal shock behavior of W-TiC-Y ₂ O ₃ composites prepared by wet chemical method.....	231
First-principles study of the effects of oxidizing medium S and additives (Hf, Pt, Y, Ce) on the adhesive behavior of matrix/oxide layer interface in austenitic heat-resistant steels.....	232
Aluminizing high silicon ductile iron by low temperature pack processing.....	233
TRD treatments in compact (vermicular) graphite cast iron.....	234
Hardness loss and microstructural evolution of 50% hot-rolled 2%-Y ₂ O ₃ dispersion strengthened tungsten at 1250-1350 °C.....	235
Effect of macrosegregation on austenite grain growth of a reactor pressure vessel steel.....	236
Application of deep ion nitriding in nuclear power equipment.....	236
The effects of thermal shock on irradiation damage behavior of W-TiC composites were prepared by wet chemical method.....	237
Microstructure and micromechanical properties of B ₄ C/Al neutron absorbing material.....	237
Microstructure and mechanical properties of Al/W-B-Al/Al laminar shielding composites prepared by SPS.....	238
Effect of stabilization treatment on hydrogen performance of high temperature heat-affected zone of TP321 stainless steel.....	238
Effects of pre-oxidation on the corrosion behavior of pure Ti under coexistence of solid NaCl deposit and humid oxygen at 600 °C.....	239
Investigation of applied stress on the corrosion behavior of 15Cr tubing in CO ₂ /H ₂ S environment.....	239
Study of mechanical properties and microstructure of air cooling bainitic steel for aluminizing tubing.....	240
Cost and resource effective surface layer heat treatment in gear and tool industry by PulsPlasma®-Nitriding.....	240

High Energy Beam Surface Engineering and Additive Manufacturing

Effect of scanning path and overlapping rate on residual stress of 316 stainless steel blade by finite element simulation of laser shock peening.....	241
Effect of SHS and SLIPS on corrosion resistance of 2219 aluminum alloy by femtosecond laser texturing.....	242

Influence of processing speed on the properties of high speed steel laser cladded deposits.....	243
The oil-water separation research in stainless steel mesh using femtosecond laser processing printer powder coated mesh.....	244
Effects of different feeding powders on microstructure and mechanical properties of 316L stainless steel repaired by laser metal deposition.....	245
Parametric investigation on supersonic laser deposition with powder mixture of Stellite-6 and tungsten carbide.....	246
δ -phase precipitation in Inconel 718 superalloy fabricated by electromagnetic stirring assisted laser solid forming.....	247
Numerical and experimental investigation on laser metal deposition as repair technology for 316L stainless steel.....	248
Research progresses on the measurement and control of laser cladding forming process.....	249
Surface textured treatment by plasma jet dispersed hardening: a potential method for improving the service life of the rail steel.....	250
Laser hybrid surface engineering—a new way to future development.....	251
Towards hard yet tough ceramic coatings.....	251
Design of titanium alloys for additive manufacturing based on cluster-plus-glue-atom model.....	252
A new technique to fabricate tin-graphite anode of lithium ion battery using laser sintering: microstructure and electrochemical properties.....	252
Heat treatment of a hot work tool steel produced by selective laser melting.....	253
The shaping and performance for wire arc additive manufacturing of advanced materials.....	253
Effects of service temperature on tensile properties and microstructural evolution of commercially pure titanium subjected to laser shock peening.....	254
Laser surface modification for the industrial and national defense applications.....	254
Microstructural control of Inconel 718 using quasi-continuous-wave laser additive manufacturing.....	255
Influence of Y_2O_3 on microstructure and cracking susceptibility of Ni-based coating fabricated by laser cladding with different fluxes of shielding and powdered gas.....	255
The influence of TiC on the microstructure and mechanical properties of carbide laser cladding.....	256
Supplier process control of laser metal deposition with coaxial nozzle.....	256
Fabrication and characterization of high strength Al-Cu-Mg alloy using directed energy deposition.....	257
Influence of laser welding temperature field on porosity of galvanized steel.....	257
Formation mechanism of femtosecond laser induced micro/nano-structure on 443 stainless steel surface under different environmental media.....	258
Design and laser additive manufacturing of Ni-based superalloys.....	258
Evaluation of interface defect in plasma transferred arc cladding process using spontaneous magnetic signals.....	259
Control of dendritic structure and crystallographic texture during laser additive manufacturing of nickel based superalloy.....	259

Investigations on microstructure and wear resistance of Fe-Mo alloy coating in situ fabricated by plasma transferred arc cladding.....	260
Drilling in inconel 718 by femtosecond laser with burst mode.....	261
Microstructure and corrosion resistance of FeCoCrNiCu high entropy alloying coating deposited by electro-spark process.....	262
Comparative study on micro arc oxidation coatings on commercially forging and selective laser melting titanium alloy.....	263
Effects of cryogenic keeping time during cryogenic laser peening process on tensile properties and micro-structure of 2024-T351 aluminum alloy.....	264
Microstructure and mechanical properties of Fe901 fabricated by electromagnetic field-assisted laser additive manufacturing.....	265
Study on mechanical properties and microstructure of laser cladged graphene nano-platelets reinforced Inconel 625 superalloy composite coating.....	266
Effects of Ni/Co on properties of aluminum bronze laser claddings.....	267
Selective laser melting of Ti-Mo based alloys.....	268
Microstructure evolution and wear behavior of in-situ synthesis boride and carbide particle reinforced Ni60CuMoW coating by combination of laser cladding and tempering treatment process.....	269
Investigation on wear resistance of nodular cast iron by laser heat treatment.....	269
Influence of metal coating on laser welding of glass.....	270
Effect of dislocation behaviors on micro-structural evolution of laser shock processed commercial pure aluminum and aluminum alloy 2A02.....	270
Investigation on the microstructure and properties of different nickel-based coatings deposited by laser cladding.....	271
Microstructure and corrosion behavior of amorphous Ni-Cr-Si-B-Fe coating fabricated by laser additive manufacturing.....	271
Stress and temperature distribution for arc weld-based rapid prototyping of titanium alloy TC4.....	272
Influences of inclination angles on microstructure and mechanical properties of 316L stainless steel parts fabricated by selective laser melting (SLM).....	272
Influence of O ₂ /N ₂ flow ratio on the microstructure and properties of AlCrON coatings deposited by multi-arc ion plating.....	273
Design of Fe-alloy/Ni-alloy multi-layered laser cladding coatings for repairing and remanufacturing GCr15 rollers.....	273
Study on structures and properties of laser surface alloying of Co-based alloyed layer on ductile iron hot roller.....	274
Study on corrosion and corrosive wear behaviors of N-doped Ni-Cr coatings deposited by arc ion plating.....	274
Corrosive wear properties of Cr ₃ C ₂ -NiCr-TiN/TiAlN duplex coatings prepared by combination of HVOF and arc ion plating.....	275

Microstructure and mechanical properties of SA336F12 fabricated by electricity melting additive manufacturing technology.....	275
Mechanical properties and corrosion behaviors of TiN/TiAlN multilayer coatings by ion source enhanced hybrid arc ion plating.....	276
The methodology research of industrial design for remanufacture.....	276
Microstructure and tensile properties of laser additive repaired titanium alloy.....	277
Effect of annealing on the microstructure properties of supersaturated Cu-Cr alloy film and bulk.....	277
High temperature oxidation behaviors of HVOF-sprayed Cr ₂ C ₃ -NiCr coating in air at 800 °C.....	278
Grain morphology evolution and texture characterization of wire and arc additive manufactured Ti-6Al-4V.....	278
The thermal fatigue behavior and cracking characteristics of ductile Ni-resist cast iron for exhaust manifolds.....	279
Influence of Al content on microstructure and properties of TC4 alloys fabricated by laser additive manufacturing.....	279
Microstructure and electrochemical anodic behavior of Inconel 718 fabricated by high-power laser solid forming.....	280
A constitutive model for high temperature deformation of AZ31 magnesium alloy.....	280
Microstructure and wear resistance of in-situ synthesized (Ti ₃ Al+TiB)/Ti composites by laser surface additive manufacturing.....	281
Localized grain boundary melting induced HAZ liquation cracking during laser solid forming of IN-738LC superalloy.....	281
The effect of micro-B addition on microstructure and mechanical properties of laser additive manufacturing Ti-6Al-4V.....	282
Mechanical properties and microstructural characterization of bronze fabricated by selective laser melting.....	282

New Technologies for Hard and Superhard Thin Films

Plasma surface niobium alloying on pure titanium surface.....	283
Simulation of residual stress of different TiN coating systems on Be substrate.....	284
Tuning the growth and surface enhanced Raman effect of graphene layers for adsorbed single molecules.....	285
Plasma spraying process and corrosion resistance of NdFeB alloy surface.....	286
Comparison in wear properties and cutting performance of TiAlN and TiAlN/MoN multilayer coatings deposited by magnetron sputtering.....	287
The growth of TiCN films by arc ion plating.....	288
Structural evolution and properties of hydrogenated W-doped DLC films.....	289
Influence of nitrogen implantation on optical properties of CVD bulk diamond and diamond films.....	292

Effect of scanning path and overlapping rate on residual stress of 316 stainless steel blade by finite element simulation of laser shock peening

Gang Xu, Fengze Dai, Jinzhong Lu
(School of Mechanical Engineering, Jiangsu University)
blueesky2005@163.com

Abstract: The effects of different paths of laser shock peening (LSP) impacts on the distribution of the residual stress in the 316L stainless steel blade were investigated by means of finite elements simulation analysis. A three-dimension analysis model subjected to LSP impacts was established by using the finite element simulation software and the distributions of LSP-induced residual stress on the surface and along the depth direction were analyzed. The 3D model of the blade with 130 mm×50 mm was drawing in UG by the command of sweeping. The process of LSP was developed with ABAQUS software, which has great advantage on explicit and implicit algorithm and thus can accurately handle transient shock wave propagation in the material. During the simulation of LSP, the shock area is treated by Multi-point shock with the square spot, the length of the square spot side is 3 mm. The shocked area is a 12 mm×9 mm rectangle area which is curving and be closed to the edge of the blade. The overlapping rate between two adjacent square spot was 50% and 70% for comparison to research the effect of the overlapping. The path 1 is an “S” type laser shock path which is advanced in the direction of the width of the blade and advancing toward the length of the blade. The path 2 is a rotary “S” type laser impact path which is advanced in the direction of the path length and advancing toward the blade width direction. Then, use the origin lab to analysis the data selected along the length and the width of the blade. The results showed that the surface compressive residual stress induced by path 1 (heading direction is along the width of the blade) was larger than path 2 (heading direction is along the length of the blade), but the distribution of surface compressive residual stress induced by path 2 was more uniform than that induced by path 1. The thickness of the residual stress induced by path 2 is deeper than path 1. In addition, with increasing overlapping rate, the distribution of the surface compressive residual stress was more uniform and the value of the surface compressive residual stress obviously increased. We can get the conclusion that LSP is a positively influence the blade and distribution of the residual stress can be affected by the laser path, the path 2 which is advanced in the direction of the path length can get the more uniform and deeper compressive residual stress than path 1 which is advanced in the direction of the width of the blade and the results apply to different overlapping rate. The change of the thickness of the blade can affect the release of the residual stress to affect the distribution. When the thickness of the blade along the laser path is constant, the distribution of the residual stress can be more uniform. To achieve the homogeneous residual stress, the chosen path of the LSP along the blade edge whose thickness is unaltered can be better.

Keywords: laser shock peening, residual stress, finite element simulation, different path of impact, 316L stainless steel

Effect of SHS and SLIPS on corrosion resistance of 2219 aluminum alloy by femtosecond laser texturing

Zexu Zhao, Lijun Song

(State Key Laboratory of Advanced Design and Manufacturing for Vehicle Body, Hunan University;
Hunan Provincial Key Laboratory of Intelligent Laser Manufacturing, Hunan University)

zhaozexu@hnu.edu.cn

Abstract: Aluminum and its alloys have been widely used in industrial fields because of their higher strength ratio, low density and good plasticity. However, corrosion of metal causes huge economic losses and limits the application of metal. Inspired by lotus leaf and nepenthes pitcher, a potential strategy was produced based on superhydrophobic surface (SHS) and slippery liquid-infused porous surface (SLIPS) to prevent metal corrosion. In this research, we fabricated a micro-nano composite structure on the surfaces of 2219 aluminum alloy by femtosecond laser texturing. Then, the superhydrophobic surface was prepared on the above structure by chemical modification with low surface energy fluorosilane. Finally, the slippery liquid-infused porous surface was fabricated on the SHS by coating lubrication perfluoropolyethers. The morphology, composition and wettability of the as-fabricated samples were characterized by scanning electron microscopy, X-ray diffraction and contact angle meter. Furthermore, the corrosion resistance properties of SHS and SLIPS in 3.5% NaCl solution were evaluated by electrochemical measurements. SEM showed that the processed by femtosecond laser texturing was regularly arranged with several 10 μm protrusions and grooves, and sub-micro spherical structures were attached to these protrusions. This micro-nano composite structure increased the roughness of the sample surface. The SHS showed excellent superhydrophobicity with the contact angle of 158.5° after fluorination. According to the Cassie model, the high surface roughness and low surface energy lead to larger contact angles. The SLIPS showed low adhesive force with the sliding angle less than 3° after using lubricant. The coarse micro-structure increases the contact area between the lubricant and the substrate, and the nano-structure enhances the capillarity, which allows the lubricant to infiltrate more easily. At the same time, oleophilic groups make the surface store more lubricant. Potentiodynamic polarization curves obtained by electrochemical measurements investigated the short-term corrosion resistance for immersing the SHS and SLIPS samples in NaCl solution for 1h. Both samples showed lower corrosion currents and higher corrosion potential than untreated sample, which demonstrated that both samples had good corrosion resistance. The air layer between the corrosion liquid and the substrate on the SHS prevented the intrusion of chloride ions, and the lubricating oil on the SLIPS was also a physical barrier to prevent corrosion. After immersion for 15 day, the corrosion rate of all the samples increased and the corrosion potential moved to left demonstrated that both air layer and lubricant slowly lose over time. Furthermore, the corrosion current density of untreated sample was higher than before, indicating that the corrosion had been occurred on the surface during the immersion the NaCl solution. The corrosion current density of SHS and SLIPS was ca.1 and ca.2 orders of magnitude lower than that of the untreated sample. From the comparison of corrosion current density and potential, the lubricant was more effective than the air layer in terms of protecting the aluminum alloy from corrosion in simulated seawater. This research provides a new method for preparing SHS and SLIPS by femtosecond laser texturing to improve the corrosion resistance of aluminum alloys.

Keywords: femtosecond laser, aluminum, corrosion, superhydrophobic, SLIPS

Influence of processing speed on the properties of high speed steel laser clad deposits

Naveed Ur Rahman¹, David Mercier², Luigi Capuano¹, David Matthews¹, Matthijn de Rooij¹, Gisele Walmag², Mario Sinnaeve³, Gert Willem Romer¹

(1. University of Twente; 2. CRM Group; 3. Marichal Ketin)

n.naveedurrahman@utwente.nl

Abstract: A comparative study is performed on high power laser cladding of two, cobalt-rich (Co-rich) and vanadium-rich (V-rich), high speed steel (HSS) alloys. The alloys were laser clad by using a 4.0 kW Nd:YAG laser source to produce defect free clad layers on a 42CrMo4 cylindrical substrate. Laser cladding was performed with off-axis powder injection relative to the propagation of the laser beam at three different laser scan speeds (5, 10 and 15 mm/s). The purpose of varying the processing speed was to investigate its effect on the microstructural refinement and mechanical properties of the laser clad deposits. Microstructural characterization of the laser clad deposits constitute studies of the matrix and carbides using scanning electron microscopy (SEM), energy dispersive spectroscopy (EDS) and electron backscatter diffraction (EBSD). Hardness measurements of the clad layers were performed by micro- and nano-indenters. Phase quantification was performed by combining nano-indentation with EBSD. Microstructural characterization reveals that the V-rich HSS alloy mainly consists of blocky V-rich primary carbides with a small contribution of angular Mo-rich carbides. The matrix consists of martensite along with retained austenite. The Co-rich HSS alloy consists of a dendritic microstructure having interdendritic networks of V, Mo and W enriched eutectic carbides, while Co remains in solid solution with iron (Fe). It is observed that Cr-rich carbides ($M_7C_3/M_{23}C_6$) are part of the matrix for both alloys and can only be observed by EBSD.

During laser cladding, the laser scan speed was varied between 5, 10 and 15 mm/s. It was found that the V-rich HSS alloy showed significant refinement in microstructure with the increase in laser processing speed. The carbide percentage increased, resulting a substantial increase in micro hardness, i.e. from 725 HV (5 mm/s) to 855 HV (15 mm/s) and a decrease of carbon content in martensite and retained austenite. The Co-rich HSS alloy showed only a marginal refinement of microstructure with the increase in processing speed, but it showed an overall higher hardness due to the presence of Co in the solid solution. The effect of multiple overlapping layers on the micro-hardness was also studied for both alloys and showed that reannealing of the previously clad layer resulted in a hardness drop in that layer.

Nano-indentations were performed by ensuring a constant maximum indentation depth of 40 nm. The results of the nano-indentation studies were mapped on the SEM micrographs, using a MATLAB script. In this way, the nano-indentations could be used in phase analysis and provided a fair comparison with EBSD results. This study therefore indicates that this novel approach in nano-indentation mapping is powerful for such investigations. Due to local hardness variations, nano-indentation was also used to distinguish between the different carbides.

Keywords: laser cladding, high speed steel, microstructural refinement, nano indentation

The oil-water separation research in stainless steel mesh using femtosecond laser processing printer powder coated mesh

Wei Wang, Xuan Liu, Lijun Song
(Hunan University)
ljsong@hnu.edu.cn

Abstract: Oil-polluted water has recently become a global challenging task due to expanding industrial oily wastewater production and frequent oil spill accidents. This pollution is a serious threat to the sea ecosystem, threatening marine life and affecting human health because the decomposition of oil contains harmful chemicals. It is of great importance to create novel technologies to separate oil and water, much of work for oil-water separation has been done for it and the most conventional way is to fabricate superhydrophilic/superoleophobic surfaces. However, most of the methods have limitations for large-scale fabrication, due to complicated processes, low commercial availability and inability to adapt to harsh environment. By observing the other species in the polluted water area, we found that many fish have the ability to resist oil soaking and live freely, and this ability is closely related to the surface structure and chemical composition of the fish scale. Researchers has shown that fish scale is multi-scale micro/nanostructures and consists of hydrophilic chemical components, this makes the fish scale superhydrophilic in the air and superoleophobic underwater.

Inspired by fish scale, we developed a novel functional material by coating printer powder (PP) on femtosecond laser treated stainless steel mesh. The stainless steel mesh was first cleaned in ethanol by ultrasonic wave at room temperature and dried in the air, and then scanned by fs laser to create hierarchical structures. Printer powder, which is formed by micro resin and sicut particles was purchased at local shop. Subsequently, they were mixed with waterborne polyurethane and acetone, and then stirred magnetically for at least 1 h to obtain a homogeneous suspension. The suspension was then sprayed onto the stainless steel mesh substrate on the untreated side with compressed air gas using a spray gum. Finally, the printer powder coating was dried at ambient temperature to allow the acetone to evaporate completely. Then the wettability of the substrates was characterized. The water contact angle of the substrate on the laser treated side was less than 10°, exhibiting superhydrophilic to water. And the other side, which was coated with printer powder has an oil contact angle for more than 150° underwater, indicating superoleophobic to oil. To test the mesh's ability of water/oil separation, a series of oils and organic solvents including kerosene, petroleum ether, hexane and chloroform were used in this study. They were mixed with water in a 1:1(v/v) ratio separately, and then were poured onto the as-prepared mesh. The separation efficiency was calculated according to $\eta=(m_1/m_0)\times 100\%$, where m_0 and m_1 are the mass of the oil before and after the separation process, respectively. The result showed good separation efficiency and fast separation speed in the experiments, and indicated excellent stability of the as-prepared mesh even in the various corrosive and active aqueous solutions, including acid, salt, base and hot water. Herein, this facile and novel machining stainless steel mesh combined with so many advantages would make it an ideal candidate for oil/water separation and even under harsh conditions.

Keywords: femtosecond laser processing, oil/water separation, printer powder, stainless mesh

Effects of different feeding powders on microstructure and mechanical properties of 316L stainless steel repaired by laser metal deposition

Guifang Sun¹, Xuting Shen¹, Zhandong Wang¹, Mingjie Zhan¹, Sai Yao¹, Rui Zhou², ¹Zhonghua Ni

(1. School of Mechanical Engineering, Southeast University;

2. School of Mechanical and Metallurgical Engineering, Jiangsu University of Science and Technology)
gfsun@seu.edu.cn

Abstract: In the present study, Ni-based alloy and 316L stainless steel powders were used to repair the T-groove on the 20 mm 316L stainless steel plate by laser metal deposition. Microstructure and mechanical properties of the repaired specimens have been compared in detail. The orthogonal trials were conducted to get optimized parameters (powder feeding rate, laser power, scanning speed, height shift). The microstructure was observed by optical microscope (OM) and scanning electron microscope (SEM), the tensile strength tested on standard dog-bond achieved according to ASTM E8M-2004, and charpy impact tests prepared in accordance with ASTM E23-02a was measured to detect the difference of the repaired specimens with two kinds of powders. The charpy impact tests were performed in the low temperature to make a comparison with the impact absorb energy at the room temperature. Moreover, the correlation between the microstructure features and mechanical properties of each repaired specimen was also analyzed.

Results indicated that the kinds of feeding powder had a huge influence on the microstructure, metallurgical bonding and mechanical properties of the repaired specimens. Microstructure of each repaired specimen under optimized parameters was dense without the evidence of pores and cracks. The microstructure of repaired zone with Ni-based alloy showed cell dendrite with different sizes while that of repaired specimens with 316L stainless steel consisted of columnar dendrites of different sizes and clusters of cells. The dimension of the dendrite was also investigated to make a further research on the morphology of the cross-section of repaired specimens. The average ultimate tensile strength of the repaired specimens with Ni-based alloy and 316L stainless steel was 94.3% and 97.2% that of the substrate (582 MPa), respectively, which reflected that the tensile strength of repaired specimens almost reached the properties of the original specimens. The absorbed impact energy at $-40\text{ }^{\circ}\text{C}$ of repaired specimens with Ni-based alloy and 316L stainless steel was 200 J and 135 J, respectively, accounting for 84% and 56.8% of the substrate (238 MPa) measured at $-40\text{ }^{\circ}\text{C}$. Obviously, impact absorb energy value of repaired specimens using Ni-based alloy was quite higher than that of repaired specimens with 316L stainless steel, which might be related to the microstructure and phases of the repaired zone of the two kinds feeding powders. As the result of the good comprehensive mechanical properties of Ni-based alloy and fine metallurgical bonding, the properties of repaired specimens increased dramatically. Besides, the mechanical properties of the specimens repaired by laser metal deposition using two kinds feeding powders exhibited enormous different characterizations related to differences in the microstructure and phases. In a word, the repaired specimens using Ni-based alloy exhibited a better comprehensive behavior than using 316L stainless steel with respect to repairing the T-groove on the 316L stainless steel by laser metal deposition under the same experiment conditions. Furthermore, both powders can be used to recover some typical mechanical properties of the broken 316L stainless steel specimens by laser metal deposition with the appropriate parameters.

Keywords: laser metal deposition, feeding powders, 316L stainless steel, Ni-based alloy, microstructure, mechanical property

Parametric investigation on supersonic laser deposition with powder mixture of Stellite-6 and tungsten carbide

Bo Li, Lijuan Wu, Xin Zhang, Qunli Zhang, Jianhua Yao
(Zhejiang University of Technology)

libo1011@zjut.edu.cn, laser@zjut.edu.cn

Abstract: In many applications, engineering parts are required to exhibit enhanced surface properties such as wear, corrosion and oxidation resistance to improve electrical, thermal and optical performance, with a view to increase the service life of such components and to reduce the frequency of downtime. Materials with these properties are usually expensive and it is beneficial to reduce cost by using cheaper bulk materials and improving the surface properties by surface modification, or applying specialized coating materials.

Metal matrix composite coatings (MMCs) composed of metal matrix and ceramic particles have received particular attention in surface engineering owing to their excellent comprehensive properties. Many processes such as laser cladding, vacuum brazing, thermal spray, cold spray, etc., have been developed to deposit a wide variety of composite materials with the desired properties onto different substrates. Among the available coating techniques, laser cladding has been the most frequently used one. Fe-, Ni- and Co-base alloy coatings reinforced with carbides and/or oxides prepared by laser cladding have been extensively reported. However, laser cladding is a high temperature process which involves rapid melting/cooling of the coating materials and the surface layer of substrate. When the clad layer consists of metal matrix composite materials, cracks are easily formed at the brittle ceramic particles due to the considerable differences in the volume change induced by the thermal expansion mismatch between the matrix and ceramic particles.

Supersonic laser deposition (SLD) is a new coating and fabrication process in which a supersonic powder stream similar to that found in cold spray (CS) impacts onto a substrate which is simultaneously heated with a laser. SLD retains the advantages of CS: solid-state deposition, high build rate and the ability to deposit metals onto a range of substrates. The addition of laser heat energy permits a change in the thermodynamic experience of impacting particles, thereby offering a greater opportunity for efficient bonding at lower velocities as compared with the CS process. Meanwhile, due to the relatively low laser energy with comparison to laser cladding, SLD will enable the coating and fabrication of engineering components with little or no melting, thus avoiding many of the thermal stress, distortion, dilution and microstructural problems associated with high temperature process.

The focus of this research is on the parametric investigations of supersonic laser deposition with powder mixture of Stellite 6 and WC. The influences of laser irradiation temperature, WC particle size and WC volume fraction on the deposition behavior and microstructures of the as-prepared MMC coatings were systematically studied. The experimental results show that deposition efficiency, WC concentration and interface bonding of the composite coatings can be effectively adjusted by altering the parameters including laser irradiation temperature, WC particle size and concentration. The results of this paper laid a solid theoretical foundation for preparation of metal-matrix composite coatings with SLD, which can be widely used in the surface modification for various metals and alloys.

Keywords: supersonic laser deposition, WC/Stellite 6 composite coating, deposition behavior, microstructure

δ -phase precipitation in Inconel 718 superalloy fabricated by electromagnetic stirring assisted laser solid forming

Feiyue Lyu
(Nanchang Hangkong University)
834221866@qq.com

Abstract: Inconel 718 superalloy samples were fabricated by electromagnetic stirring assisted laser solid forming (EMS+LSF). Inconel 718 alloy can improve the plasticity and improve the notch sensitivity when it contains the appropriate amount of δ phase. In the process of forging and heat treatment of Inconel 718 alloy, it is likely to dissolve the precipitated δ phase partially or completely. If the process is not controlled inappropriately, the austenite grain size will be large and then the alloy will show the poor notch sensitivity. Therefore, it is necessary to change the number of δ phase by different heat treatment system and the intensity of different magnetic field to improve the performance of the alloy. Meanwhile the precipitation behavior of δ phase in samples deposited with various magnetic field intensities during heat treatment at different temperatures were experimentally investigated. It is shown that under the action of magnetic field, the microstructure and the distribution of Nb elements in LSF Inconel 718 superalloy changed due to the intense convection of liquid metal in the molten pool. After heat treatment, the size, morphology and volume fraction of δ phase show obvious influence by the magnetic field intensities. The solidification microstructures of LSF Inconel 718 superalloy with different magnetic field intensity and different heat treatment were observed by metallographic microscope (OM), scanning electron microscope (SEM), energy spectrum (EDS), and its mechanical property were tested. With the increase of the magnetic field intensity from 0 mT to 80 mT, the length of δ phase declined from 1.14 μm to 0.99 μm in aging 1 h, from 1.36 μm to 1.05 μm in aging 4 h, and from 1.40 μm to 1.13 μm in aging 16 h. Then the width of δ phase grew up slightly between 0.070 μm and 0.075 μm in aging 4 h and 16 h, while the width of δ phase decreased first from 0.103 μm to 0.083 μm before 30 mT, and after that increased slightly from 0.083 μm to 0.089 μm . The length-to-width ratio of δ phase increased when the magnetic field intensities were in range of 0 mT and 50 mT, and then decreased when the magnetic field intensity went on increasing. However, the volume fraction of δ phase in different aging time had different trend. In other words, the fraction of δ phase reached its largest amount of 9.36% after aging at 950 °C for 4 hours and 10.70% for 16 h when the magnetic field intensity was 30 mT, while there was a obvious decline from 5.80% to 2.43% for 1 h when the magnetic field intensity reached 30 mT. After that the fraction of δ phase hold steady when the magnetic field intensity exceeded 50 mT. The hardness measurement of the heat treated samples shows rapid increasing of microhardness with the increase of magnetic field intensity. To be specific, when the magnetic field intensity went up from 0 mT to 80 mT, the figure of microhardness also increased from 297.7 HV to 363.16 HV in aging 1h, from 285.66 HV to 386.49 HV in aging 4 h, and from 279.69 HV to 343.11 HV in aging 16 h. So with the increase of magnetic field strength, the fraction of δ phase is reduced on the whole, while the hardness of the alloy increases.

Keywords: electromagnetic stirring assisted, laser solid forming, inconel 718 superalloy, δ phase, precipitation regular

Numerical and experimental investigation on laser metal deposition as repair technology for 316L stainless steel

Mingjie Zhan, Guifang Sun, Zhandong Wang, Xuting Shen, Sai Yao, Zhonghua Ni
(School of Mechanical Engineering, Southeast University)
gfsun@seu.edu.cn

Abstract: In this study, laser metal deposition technology was used to repair 316L stainless steel plate of 20 mm thickness with a dovetail groove using 316L stainless steel powder as raw material. The dovetail groove was repaired by six successive metal layers. To give a better insight of temperature field distribution of the molten pool which was difficult to be monitored by experiment methods during laser metal deposition, numerical methodology (finite element method) was used to predict the thermal behavior to make comparison with the experimental results. Laser beam was simulated as a heat source model with a Gaussian distribution. Element birth and death technology in the finite element software ANSYS was used to simulate the metal deposition. This investigation focused on the influence of adjacent track (the second track in the first layer and the first track in the second layer) processing on the first track in the first layer. The influence was reflected by measuring the cross-sectional micro-hardness and microstructural evolution in the first track in the first layer. The development of molten pool during laser metal deposition was also studied.

The numerical results indicated that the maximum temperature and dimensions of the molten pool increased as the deposition in progress. The laser beam melted the previous layer surface thoroughly when subsequent layer was deposited, thus forming a fine metallurgical bonding between adjacent layers. The first track in the first layer can experience a peak temperature after the deposition of the second track in the first layer and the first track in the second layer. The thermal cycling caused by the peak temperature produced a significant effect on the microstructure of the first track in the first layer. The temperature field distribution of molten pool was used to analysis the variation of microstructure in the first the track in the first layer. The microstructure of the deposition was revealed by a scanning electron microscope which showed good metallurgical bonding. The microstructure of the first track in the first layer mainly included columnar dendrites which grew epitaxially from the molten pool boundary and a few cluster of cell dendrites distributed in the interface. The interface between the first track in the first layer and the substrate showed no clear planar band. The differences among the microstructure of the first track in the first layer in different processing situations (the first track in the first layer, the second track in the first layer and the first track in the second layer) mainly lay in the grain sizes and shapes. The average micro-hardness of the first track in the first layer measured along the central vertical direction of the molten pool exhibited a few fluctuation among the three situations (197.23, 209.89 and 201.3 HV).

The simulated temperature history was compared with the experimental measurements acquired by a K-type thermal-couple located in the surface of the substrate. The metallographic structure of the repaired zone had a good agreement with the numerical results, indicating the validity of the numerical methodology.

Keywords: laser metal deposition, finite element simulation, 316L stainless steel, thermal cycling, microstructure

Research progresses on the measurement and control of laser cladding forming process

Yali Qiao, Jianli Song, Haiyang Li, Xiaolei Shi
(Beijing Information Science and Technology University)
songjianli@bistu.edu.cn

Abstract: Laser cladding forming (LCF) is a novel advanced manufacturing technology in which three dimensional full density components with excellent corrosion and wear resistance can be obtained. In the process of LCF, factors such as the temperature field of the molten pool, geometrical morphology of the cladding layer and deformation and cracks of the formed component has a significant influence on the forming performance of the components. Via the measurement and control of these important information and parameters, quality and characteristics of the cladding layer can be predicted and guaranteed. Therefore, measurement and control of the LCF process become a hot spot in the research field of laser material processing and forming.

The measurement and control of the molten pool temperature, geometrical morphology of the molten pool and cladding layer, and forming defects in the process of LCF has been reviewed. Several measurement and control systems and methods have been summarized and analyzed, and the future prospect and development trends have also been proposed, which will provide a reference for the future research and development of the LCF process.

For the signals of the temperature field, geometrical morphology and defects detection, non-contact vision measurement methods with the assistant of cameras have gradually become the main approaches due to their unique advantages. And during the detection process, real time detection and closed-loop control of the multiple signals have become the main trends, and the quality of the cladding layer can be significantly improved by controlling of the cladding process parameters. Besides, the detection and research of cooling rate has constructed a close correlation with the microstructure of the cladding layer, which represents that further exploration of other effective signals of the molten pool is an important research direction to improve the quality of the cladding layers. For the control system, with the continuous improvement of control algorithms, application of layer-to-layer control method and development of new algorithm implementation platform such as FPGA (field-programmable gate array) and LabVIEW, striding forward of the control system is obtained in aspects of stability, accuracy and real-time characteristics. As a result, the homogeneity, precision and property of the cladding layers have also been greatly enhanced.

The main role of the detection and control of the molten pool temperature and geometrical morphology is to reduce the macroscopic defects such as deformation and cracking. It is also one of the focuses of the research on defect detection and control technology in the LCF process at home and abroad. However, the method is unable to detect the defects such as micro crack and lack of fusion in the cooling of the melt channel, which has not been effectively solved so far. It is hoped that the method can be further improved in the control of the part precision, and breakthrough of internal defect detection and control also be carried out.

Novel design and manufacturing methodology such as integrated Material-Structure-Performance forming is one of the development frontiers to enlarge the application the LCF and improve the quality of the process by utilizing fit materials in fit positions. With the development of new LCF technology such as Hybrid Additive-Subtractive manufacturing and novel measurement, sensing and control methods, the forming quality of the LCF components will be further improved and the application of this process will the further expanded.

Keywords: laser cladding forming (LCF), molten pool, cladding layer, defects, measurement and control

Surface textured treatment by plasma jet dispersed hardening: a potential method for improving the service life of the rail steel

Yazhou Duan, Deping Yu, Yong Xiang, Jier Qiu, Xin Zhou, Jin Yao
(School of Manufacturing Science and Engineering, Sichuan University)
williamydp@scu.edu.cn

Abstract: With the development of heavy load and high-speed railway, the life of the rail has become one of the key problems in railway transportation. In order to ensure the contact fatigue resistance (CFR) of the rail, the hardness of rail is limited to HB400 in modern technical standards, which limits the improvement of the wear resistance of the steel rail by the traditional heat treatment methods.

To improve the wear resistance and maintain the CFR of the rail, a surface textured treatment (STT) based on plasma jet dispersed hardening was proposed to strengthen the rail. For the high energy density of the laminar plasma jet, the microstructure of the heated regions can change from pearlite to lath or acicular martensite and retained austenite in a very short time. The hardness of these regions hardened was found to reach up to 770-950 HV0.1. By properly designing the shapes and sizes of these regions, the wear resistance of the rail steel was greatly improved and the CFR is maintained.

To reveal the effect of STT on the rolling/sliding wear behavior of the rail steel, rolling contact wear tests were carried out on an Amsler twin-disc rolling/sliding testing machine according to the Chinese standard GB 12444.1-90. To simulate the actual contact between the wheel and the rail, the loading force was calculated by Hertz elasticity contact theory to ensure the same contact stress as the real situation. Laminar plasma jet was used to create a textured surface with different shapes, e.g. circular spot with different sizes, teardrop spot, single channel etc., on the rail steel roller. Rolling contact wear tests were carried out using the treated and untreated rail steel rollers. The wear tests were broke off at every 20,000 cycles to measure the weight losses. At the end of the tests, the rail rollers were sectioned for metallographic observation using optical microscope (OM) and scanning electron microscope (SEM).

Experimental results showed that plasma surface textured treatment can effectively improve the rolling contact wear resistance of railway steel. The stable wear rates of the treated rail roller were reduced by around 30%-55%. Furthermore, with an increase of the ratio of the hardened regions, the wear resistance of railway steel was better. To analyze the wear behavior, the microstructure of the worn surfaces was observed by OM and SEM. It was found that the textured hardened regions bring about three effects, i.e. supporting effect, blocking effect and distribution effect to the rail steel. These effects greatly suppressed the plastic deformation of both the treated and untreated regions of the rail steel, inhibiting the formation of severe delaminating wear of the rail steel. Due to the dispersion of textured hardened regions, the phenomenon of catastrophic destruction appeared in the rail roller with the whole surface hardened was avoided. In other words, the CFR of the textured surface was maintained to be similar to that of the untreated ones. Therefore, the proposed method is a promising for improving the service life of the rail steel.

Keywords: surface textured treatment, rail steel, laminar plasma jet, wear resistance

Laser hybrid surface engineering—a new way to future development

Volodymyr Kovalenko¹, Jianhua Yao²

(1. National Technical University of Ukraine; 2. Zhejiang University of Technology)

kovalenko.volodymyr@hotmail.com

Abstract: Many problems may be reduced or even eliminated by development and implementation of advanced technologies – laser is being one of the most promising. This is especially true for time saving thanks to the fact that almost all factors at such technologies may be digitized, measured and kept under precise control. Laser surface engineering is a unique way for remanufacturing - creating the new product from used products. Manufacturer can potentially save between 60% to 90% in terms of energy, materials, water and air pollutant emissions by remanufacturing an end-of-life product (worn off, broken, damaged components or modernized design), compared to manufacturing a new product. This makes remanufacturing a green and high value-add industry with enormous growth potential. Laser surface engineering, as a representative of advanced manufacturing approaches, will inevitably transform from traditional single material, single performance and single energy field into composite materials, functional gradient and multi-energy field, and then complete the process which the traditional laser manufacturing cannot achieve. Combining electromagnetic field, kinetic energy field, ultrasonic energy field, thermal field, chemical reaction, etc. with laser surface engineering can avoid the shortcomings of single laser technology, and is able to obtain hybrid manufacturing methods with higher precision, higher efficiency, and more intelligent. Laser hybrid surface engineering (LHSE), as an international research hot spot, has gradually transformed from laboratory fundamental researches into industrial applications. With continuous innovations and breakthroughs in this field by the scholars around the world.

In this presentation, based on the review of the global research status on the LHSE, the recent research results in the field of LHSE, including the electric magnetic–laser hybrid manufacturing, the supersonic laser deposition and the electrochemical–laser hybrid manufacturing, etc., are introduced. The advantages of the LHSE are analyzed on the aspects of the material, the structure and the property. Furthermore, the challenges and solutions of the LHSE regarding the efficiency, the performance, the cost and the intelligentization are thoroughly analyzed and discussed from the viewpoints of both fundamental research and industrial application. Finally, the future trends of the LHSE are prospected.

Keywords: laser hybrid surface engineering, remanufacturing, multi-energy field

Towards hard yet tough ceramic coatings

Sam Zhang

(Southwest University, Chongqing, China)

samzhang@swu.edu.cn

Abstract: Over the past decades, hard and super hard ceramic coatings have been developed and widely used in various industrial applications. Meanwhile, an increasing number of studies have realized that the toughness is just as crucial, if not more than hardness especially for ceramic coatings. However, hardness and toughness do not go naturally hand in hand. In other words, hard coatings usually are brittle and less durable while toughened coatings are of lower strength. For practical engineering applications, it is more desirable to have coatings with high hardness without sacrificing toughness too much. In this talk, view is presented on continuous progress to realize hard-yet-tough ceramic coatings from an angle of hardening as well as toughening.

Keywords: hard and super hard ceramic coatings

Design of titanium alloys for additive manufacturing based on cluster-plus-glue-atom model

Xiaohua Min, Tianyu Liu, Cunshan Wang, Chuang Dong
(Dalian University of Technology)
minxiaohua@dlut.edu.cn

Abstract: Additive manufacturing have been conducted extensively on the basis of traditional metallic materials for achieving the high performance, while they are used suitably for common manufacturing process without considering the special features of this technique. Control of shape and property is severely restricted for traditional metallic materials during additive manufacturing process. Therefore, it is essential to develop novel materials with excellent compatibility between melt and solid structure, meaning that the stable chemical short-range-order is present from melt to solid. Thus, the metallic materials with compositions of congruent melting point in terms of phase diagrams are suitable in principle for additive manufacturing. However, the chemical short-range-order structural unit of congruent melting point still remains unclear. Thus, the cluster-plus-glue-atom model is introduced firstly to describe the chemical short-range-order structural unit of congruent melting point on the view of typical binary phase diagrams of titanium alloys, for example Ti-V, Ti-Al, Ti-Zr alloys, and to give their corresponding composition formulas. Similarity, the chemical short-range-order structural unit of industrial Ti-6Al-4V alloy is also analyzed for fine adjustment of alloying elements to further enhance its additive manufacturing properties. An effective guidance for design of additive manufacturing titanium alloys is desirable based on cluster-plus-glue-atom model.

Keywords: titanium alloys, additive manufacturing, cluster-plus-glue-atom model, congruent melting point

A new technique to fabricate tin-graphite anode of lithium ion battery using laser sintering: microstructure and electrochemical properties

Xue Zhang, Cunshan Wang
(Key Laboratory of Materials Modification by Laser, Ion and Electron Beams)
zhangxue_4900399@126.com

Abstract: In the present work, tin-graphite anode of lithium ion batteries was developed and fabricated using laser sintering on the current collector copper. The microstructure and electrochemical properties of the anode was investigated in detail. The results showed that the morphology of the graphite develops from block-shape into graphene-like during laser sintering, on which tin nanoparticles embedded. Meanwhile, the anode exhibits a good interface bonding with the current collector, owing to inter diffusion between the both. As a result, the first columbic efficiency of the anode reaches 68.8%, much higher than that (42.3%) of the anode without laser sintering. Moreover, the studied anode has a high capacity of 519.4 mAh g⁻¹ after 500 cycles charge/discharge process, when the voltage window is in the range of 0.01-2.00 V (vs. Li⁺/Li) and the current rate is 0.1 A g⁻¹.

Keywords: laser sintering, lithium ion battery, tin-graphite anode, microstructure, electrochemical property

Heat treatment of a hot work tool steel produced by selective laser melting

Massimo Pellizzari¹, Faraz Deirmina¹, Nicola Peghini¹, Bandar AlMangour², Dariusz Grzesiak³

(1. University of Trento; 2. Harvard University; 3. West Pomeranian University of Technology)

massimo.pellizzari@unitn.it

Abstract: The ever increasing demand of parts produced by additive manufacturing, has led to the need of a deeper understanding of the attainable microstructure. Special emphasis should be paid to the following heat treatment, which must take into consideration the rapid solidification structure produced by high energy beam technologies, like selective laser melting (SLM). It is now widely accepted that the optimum properties mix can be obtained only after a proper selection of the processing parameters and procedures.

Aim of this paper is to investigate the heat treatment of a hot work tool steel (AISI H13) produced by SLM. In the as-built condition the steel density is close to the theoretical one (94%). The metallographic cross section obtained perpendicularly to the building direction clearly highlights the layers sequence. The solidification structure is quite fine and irregular, being characterized by segregation phenomena and by uneven microhardness values inside the single layer. This last effect is due to the thermal changes induced by the laser beam leading to partial remelting and quenching of the outermost layer region and the uncontrolled tempering of its bottom region. The fraction of retained austenite determined X-ray diffraction is 20vol% but, due to the thermal/composition gradient its distribution is quite inhomogeneous inside the single layer. Technically, the part could be held in the as-quenched state and could undergo only multiple tempering, as provided for conventionally produced tool steels. In practice, an intermediate quenching process is found to be effective in modifying the solidification structure due to the formation of new austenite grain, even if a true chemical homogenization will not occur. After quenching, the steel microstructure does not show anymore the traces of the deposition sequence and the inhomogeneity due to thermal gradients originated by SLM disappear. The amount of retained austenite falls below 2vol%, so that the situation is greatly improved looking to the final tempering process. The tempering curves of the steel directly tempered and further quenched after SLM are significantly different, justifying the use of different parameters to get the desired hardness and properties.

Keywords: tool steel, selective laser melting, additive manufacturing, quenching, tempering

The shaping and performance for wire arc additive manufacturing of

advanced materials

Xizhang Chen

(Wenzhou University)

Abstract: The self-developed robot based wire arc additive manufacturing system is introduced. Two main key technologies to control the surface shaping and performance including mechanical properties, residual stress are introduced. The theory of phase transformation dilation is proposed to offset some or all heat shrinking when metal cooling and further reduced the tensile residual stresses. The results on the additive manufacturing of Q690 show that the residual tensile stress at weld zone by self-developed wire with low temperature phase dilation is -257.6 MPa, it is obviously reduced compare to residual stress of 175.5 MPa get by traditional wire ER110S-G. The application and additive manufacturing of other advanced materials of aluminum, copper, nickel based metal also are introduced.

Keywords: wire arc additive manufacturing, shaping and performance

Effects of service temperature on tensile properties and microstructural evolution of commercially pure titanium subjected to laser shock peening

Haifei Lu, Kaiyu Luo, Liujun Wu, Chengyun Cui, Jinzhong Lu
(Jiangsu University)
jzlu@mail.ujs.edu.cn

Abstract: Effects of service temperature on the tensile properties and microstructural evolution of tensile specimens manufactured by commercial pure (CP) titanium subjected to laser shock peening (LSP) were investigated. Special attention was paid to the microstructural features at the top surface close to the fracture zone of the failed LSPed specimens at 20, 150, 250, and 350 °C by means of transmission electron microscopy (TEM) observations. Results indicated that the ultimate tensile strength (UTS) of LSPed specimens gradually decreased, but the area reduction and elongation of LSPed specimens increased with the increment of service temperature. Furthermore, the influence mechanism of service temperature on the microstructural evolution of the LSPed CP titanium consisted of two modes: (a) ultra-high strain rate inhibited the dislocation motion at a lower temperature which was more prone to the occurrence of deformation twinning, and (b) ultra-high strain rate was easier to activate dislocation motion at a higher temperature, making deformation twinning disappear in the plastic deformation layer of CP titanium.

Keywords: laser shock peening, commercial pure titanium, temperature, tensile property, TEM observation

Laser surface modification for the industrial and national defense applications

Yan Shi
(Changchun University of Science and Technology)
shiyang@cust.edu.cn

Abstract: Laser surface modification is to use a laser beam to heat the workpieces' surface very quickly and change the structure of the material surface, so that the physical, chemical and mechanical properties of the material surface can be changed. This technology can improve the wear resistance, corrosion resistance and fatigue resistance of parts to meet different requirements, so it has been widely used in industry and national defense fields. This report mainly introduces the research and application works done by the speaker in this field. It mainly includes laser transformation hardening, laser sintering, laser cladding and laser impact hardening and so on. The laser transformation hardening treatment of the parts such as gears, cams and machine guide rails can obviously improve the wear resistance with a smaller deformation. The laser surface heat treatment of copper based powder metallurgy friction material can significantly improve the heat resistance and wear resistance of friction disk. The laser cladding, which takes engine injection valve seat and camshaft as the representative parts, improves the wear resistance, through solving the technical problems of large surface area parts and small parts with high hardness and multiple pores, and improves the wear resistance. Laser peening on the weld surface can significantly improve the corrosion resistance.

Keywords: laser surface modification, laser transformation hardening, laser surface heat treatment, laser cladding

Microstructural control of Inconel 718 using quasi-continuous-wave laser additive manufacturing

Lijun Song^{1,2}

(1. State Key Laboratory of Advanced Design and Manufacturing for Vehicle Body, Hunan University;
2. Hunan Provincial Key Laboratory of Intelligent Laser Manufacturing, Hunan University)
ljsong@hnu.edu.cn

Abstract: Solidification microstructure plays a crucial role in determining the performance of additively manufactured components. However, effective efforts to obtain on-demand control of solidification microstructure are still lacking. In this work, a quasi-continuous-wave laser additive manufacturing (QCW-LAM) was proposed to control the solidification microstructure. The results show that the QCW-LAM is characterized by an unconfined solidification process, a dynamic solidification condition (including solidification parameters and molten-pool boundary) and a periodic re-melting of molten pool. The dendritic structure is refined and the element segregation is significantly reduced in QCW-LAM due to the high cooling rate and solidification rate of the molten pool. In addition, both highly orientated columnar grains with a strong fiber texture and the randomly distributed grains with a weak cubic texture were produced by modulating the laser parameters. These microstructural characteristics are correlated with the solidification parameters in an unconfined solidification process, residual molten-pool geometry and periodic re-melting of molten pool. Further, the functionally gradient component with site specific, on-demand microstructure and performance was successfully fabricated by a customized process using a modulated laser. This work not only provides a novel method to precisely control the solidification microstructure, but also provides a valuable understanding for solidification during QCW-LAM.

Keywords: additive manufacturing, quasi-continuous-wave laser, microstructure, segregation, crystallographic texture

Influence of Y_2O_3 on microstructure and cracking susceptibility of Ni-based coating fabricated by laser cladding with different fluxes of shielding and powdered gas

Yunfeng Li, Yan Shi, Jia Liu

(Changchun University of Science and Technology)
lasercust@hotmail.com

Abstract: In the paper, Ni45 alloy composite coating was produced by laser cladding on 42CrMoA alloy steel using the 5 kW CO₂ laser, four-axis CNC machines and the co-axial powder feeding system. The influence of Y₂O₃ about microstructure and cracking susceptibility of the composite coating were investigated on the different fluxes of shielding gas and powdered gas. The macro-morphology and microstructures were characterized by using laser microscope, SEM, XRD and microhardness tester. The results show that the cracking susceptibility of the composite coating gradually decreased with the flux of shielding gas increased, when the Y₂O₃ addition is 0.4wt%. Meanwhile, the cracking susceptibility of change decreased as the flux of powdered gas increased initially and increased afterwards. The smallest cracking susceptibility and refined microstructure of the composite coating were obtained under conditions of 15 L/min of shielding gas and 500 L/h of powdered gas.

Keywords: laser cladding, Y₂O₃, cracking susceptibility, microstructure

The influence of TiC on the microstructure and mechanical properties of carbide laser cladding

Xiangwen chen
(Fujian Agriculture and Forestry University)
541048212@qq.com

Abstract: To explore the influence of the important hard phase TiC on the microstructure and mechanical properties of carbide laser cladding, carbide powder with different levels of TiC was cladding by the preset powder method, and the sample was analyzed by scanning electron microscopy (SEM), micro-hardness, wear resistance and other methods. The results showed that: Under laser rapid prototyping conditions, in addition to generate solid solution with WC, TiC will grow up together to form a black grains by itself when its mass fraction reached a certain level. With the increase of the mass fraction of TiC, the role of solution strengthening and the second phase strengthening of cladding enhanced. Microhardness increased gradually and reached a maximum when the mass fraction of TiC was 25%. Abrasive wear was the main wear mode of cladding. The friction coefficient was the most stable when the mass fraction of TiC was 15%.

Keywords: TiC, laser cladding, microstructure, wear resistance

Supplier process control of laser metal deposition with coaxial nozzle

Liqun Li¹, Yiche Huang¹, Chen Hong²
(1. Harbin Institute of Technology; 2. Fraunhofer ILT)
liliquin@hit.edu.cn

Abstract: Laser metal deposition (LMD) technology has been widely used to the industry for laser additive manufacturing, cladding or repairing the metallic parts. The quality and efficiency of laser deposition heavily depends on the supplier process control. For some special laser deposition processing, such as ultra-high-speed laser cladding, inside laser cladding, FGM and MMC coating or parts manufacturing, the power stream controlling become more complex, because the powder melting behavior is changed and varying proportion mix powder is used. In order to achieve the best feeding properties and highest deposition efficiency, the optimization of the nozzle geometry and controlling of powder flow are quite necessary. The purpose of this work is to develop an analytical foundation for fundamental understanding of heat and mass transfer, molten metal flow and free surface evolution, and achieve the supplier process control for different LMD application requirement. The numerical simulation and digital image are combined to investigate the powder convergence, molten pool physics and powder catchment efficiency.

Keywords: laser metal deposition, powder stream, coaxial nozzle concentration, numerical simulation

Fabrication and characterization of high strength Al-Cu-Mg alloy using directed energy deposition

Tao Gu, Bo Chen, Caiwang Tan, Jicai Feng
(Harbin Institute of Technology)
chenber@163.com

Abstract: As an advanced manufacturing technology, 3D printing is a new option for saving materials, shortening processing time, forming complex structures and reducing the weight of structures. Aluminum alloys have been extensively researched because of the higher strength to weight ratio than conventional steel. Laser based direct energy deposition (DED) process has been used to build up solid thin wall samples using commercial gas atomization Al 2024 powder. The effects of unidirectional laser scanning deposition and two-way scanning deposition on quality were compared. The evolution of macro- and microstructures of laser deposited Al 2024 samples was investigated using X-ray diffraction (XRD), optical microscopy (OM), scanning electron microscopy (SEM) and electron backscattered diffraction (EBSD) techniques. Microstructural observation revealed that the morphology and the width and length scale of the microstructure were different at different locations. It was observed that a periodic transition of microstructural morphology from coarse columnar grain to fine columnar grain appeared in each layer. These differences were due to the effect of heat treatment caused by the thermal cycling.

Keywords: Al 2024, DED, microstructure, thermal cycling

Influence of laser welding temperature field on porosity of galvanized steel

Lei Huang, Xizhang Chen
(Wenzhou University)
chenxizhang@wzu.edu.cn.

Abstract: It simulated the thermodynamics in the welding process using SYEWELD simulation software for DP780 galvanized dual phase steels for vehicles. First, it studied the influence of the temperature field on the formation of the welding pores. Then, based on the simulated process parameters, a process test was performed. Finally, the simulated pore morphology, weld morphology, and process test results were compared. The results show that the effect of welding simulation temperature field on the porosity is to increase the stability, and finally reduce the gradual process. The simulated porosity and process test results are similar, and the simulated weld dimensions and the experimentally derived dimensions are more similar. When changing the reserved gap from 0.3 mm to 0.25 mm, the porosity of the weld decreased by 60%, and the width of the weld was reduced by 53%.

Keywords: laser welding, galvanized steel, porosity, welded joints, welding simulation

Formation mechanism of femtosecond laser induced micro/nano-structure on 443 stainless steel surface under different environmental media

Zeqin Cui
(Taiyuan University of Technology)
cuizeqin@tyut.edu.cn

Abstract: Fs laser surface micro/nano-structuring can induce a variety of micro/nano-structures on solids' surface. It is one of the most important application areas of fs laser micro/nano-machining, and it is also an important method to fabricate functional materials with special surface properties, such as superhydrophobic surface, anti-reflection surface, etc. Thus, fs laser surface micro/nano-structuring has important application potential in photonics, nano/microfluidics, optofluidics and so on. However, the morphological optimal control of fs laser surface micro/nano-structuring and exact formation mechanisms of fs laser-induced surface micro/nano-structures are not yet fully understood and lack systematic study. Understanding exact formation mechanisms of fs laser-induced surface micro/nano-structures is crucial for fs laser surface micro/nano-structuring to controllably fabricate functional surfaces.

In this manuscript, the study of fs laser micro/nano-structuring on TTS 443 ferritic stainless steel surface in air, water and methanol was conducted. A variety of fs laser-induced surface micro/nano-structures were formed on 443 stainless steel surface via single or multiple raster scans and their formation mechanisms were discussed, which would help lay a foundation for further study on controllable fabrication of function surfaces via fs laser surface micro/nano-structuring.

It was found that Linked nano-structure-textured mound-shaped microstructures (termed N-mounds) were induced by fs laser on 443 stainless steel surface in air via multiple raster scans; In water, fs laser induced periodic surface structures were formed and their formation can be explained by the interference between incident laser and surface plasma polaritons. In methanol, with the increasing of scanning number, ripples-textured micro protrusions formed, which was the result of multi-ablation evolution and caused by inhomogeneous absorbed laser intensity distribution due to the diffraction of surface roughness. The difference in surface morphology obtained in different environmental media was caused by the difference in physiochemical properties between environmental media.

Keywords: femtosecond laser, micro/nano-structures, formation mechanisms, stainless steel

Design and laser additive manufacturing of Ni-based superalloys

Qun Yu, Cunshan Wang
(Dalian University of Technology)
laser@dlut.edu.cn

Abstract: A "cluster-plus-glue-atom" model was introduced to design Ni-Al-Cr-Nb-Ti-Mo superalloys. According to function and mixing enthalpies of alloying elements, the model specific to the Ni-based superalloys was proposed as $[Al-Ni_{12}] Al_xM_y$. When the alloys conforming to the composition formula were produced by laser additive manufacturing on pure Ni substrate, a hypoeutectic structure consisting of primary γ -Ni solid solution and (γ Ni+laves) eutectic was obtained. With the increasing contents of Cr and Mo, volume fraction of laves eutectic phase decreases, which not only reduces the cracking susceptibility of the alloys, but also enhances the high temperature oxidation resistance, mechanical and tribological properties.

Keywords: laser additive manufacturing, Ni-based superalloy, microstructure, property

Evaluation of interface defect in plasma transferred arc cladding process using spontaneous magnetic signals

Zhengchun Qian, Haihong Huang, Lunwu Zhao, Gang Han
(Hefei University of Technology)
huanghaihong@hfut.edu.cn

Abstract: During the process of remanufacturing, the defect may occur at the interface between cladding coating and substrate because of process instability or environmental interference. In order to ensure the repair quality of remanufactured product, a novel nondestructive testing method based on spontaneous magnetic signals is used to characterize the interface defect in plasma transferred arc cladding process. In the experiment, different sizes of interface defect were prefabricated by corroding substrate surface at particular areas. Then, the specimens were tested under static tensile stress; and the variation of magnetic signals was investigated during the tests. Experimental results showed that the peak width W_p of magnetic signals can reflect the location and size of interface defect; and the peak value H_p of magnetic signals increased exponentially with the increase in tensile stress. The morphology and microstructure were observed at the location of fracture and it was found that the corrosion led to the high stress concentration, which was response for the degradation of material performance and the distortion of magnetic signals at interface defect.

Keywords: interface defect, spontaneous magnetic signals, plasma transferred arc cladding, evaluation, remanufacturing

Control of dendritic structure and crystallographic texture during laser additive manufacturing of nickel based superalloy

Hui Xiao, Lijun Song
(Hunan University)
xiaohui1113@hnu.edu.cn

Abstract: Dendritic growth and crystallographic texture evolution during solidification in laser additive manufacturing (LAM) is critical for material performance and its has fascinated materials scientists for a long time. However, effective efforts to control the dendritic growth and crystallographic texture during solidification in LAM are still lacking. In this work, the periodically remelting of molten pool during LAM is introduced using the quasi-continuous wave (QCW) laser to control the dendritic microstructure and crystallographic texture and its formation mechanism is also investigated. The results shown that the high pulse frequency favored the formation of fine columnar dendrites and highly orientated crystallographic texture, while the low pulse frequency tended to produce fine equiaxed dendrites and more random crystallographic texture. The significantly modified solidification conditions and the periodic remelting of molten pool contributed to the formation of columnar dendrite and highly orientated crystallographic texture. This work reports a route to control the dendritic growth and crystallographic texture during LAM.

Keywords: laser additive manufacturing, quasi-continuous-wave laser, Ni-based superalloy, dendritic growth, crystallographic texture

Investigations on microstructure and wear resistance of Fe-Mo alloy coating in situ fabricated by plasma transferred arc cladding

Xinke Deng
(Xi'an University of Technology)
dengxinke520@163.com

Abstract: Iron-based alloys are a kind of the most widely used metallic materials for many moving mechanical components, because of their adequate strength, good ductility and toughness. However, iron-based alloys exhibit poor wear resistance when they are subject to severe abrasion and adhesion service conditions. Surface engineering technology is an effective approach to improve the wear resistance of these components by depositing a wear-resistant coating on the surface. Among the various surface engineering technologies, the plasma transferred arc (PTA) cladding is one of the most efficient surface technologies due to its advantages of high temperature (over 10,000 °C), excellent arc stability, and low dilution rate of the substrate. T. Murakami et al. found that Fe-Mo intermetallic compounds exhibited low friction coefficients and high wear resistance when sliding against AISI 52100 steel balls under lubrication. Meanwhile, they also indicated that the outstanding tribological properties were ascribed to the formation of low friction MoO₃ on the wear tracks. Therefore, Fe-Mo intermetallic compounds are expected to be promising candidates for wear-resistant coating materials. Because of their intrinsic brittleness at room temperature, it is easy to cause fracture during sliding wear process, resulting in the decrease of wear resistance. To solve this problem, it may be necessary to develop a FeMo alloy coating including ductile phase. Although a low dilution of the substrate is usually desired in the PTA cladding process, this work introduces the counter thinking design of increasing the dilution of the steel substrate by increasing the current density to in situ produce a certain amount of ductile-Fe phase in the Fe-Mo alloy coating. In this paper, the PTA cladding process was adopted to in situ fabricate a Fe-Mo alloy coating on the AISI 1045 steel substrate. The microstructure and phase composition of the coating were investigated in detail. And the wear resistance of the coating was evaluated under dry sliding wear test condition against ZrO₂ disc at room temperature. The experiments were carried out on a home-made T-600A machine equipped with a powder feeding system. The AISI 1045 steel (normalization state, original microhardness 185 HV0.3) with dimensions of 150 mm×50 mm×20 mm was employed as the substrate material. Commercial Mo powders (purity 99.9%) were selected as feedstock powders. A wear-resistant Fe-Mo alloy coating was in situ fabricated on the AISI 1045 steel substrate by plasma transferred arc (PTA) cladding, using pure Mo powders as the precursor material. The microstructure, microhardness and wear resistance of the coating were investigated by scanning electron microscope (SEM) with energy dispersive spectrum (EDS), X-ray diffraction (XRD), Vickers hardness and pinon-disk wear testers, respectively. It was found that the coating presented rapidly solidified microstructure mainly consisting of cellular R-Fe₆₃Mo₃₇ dendrites and a small amount of lamellar R-Fe₆₃Mo₃₇/-Fess dendrites uniformly distributed in the -Fess matrix. Based on the eutectic growth and undercooling theories, the possibility of the R/ peritectic coupled growth in the rapidly solidified peritectic Fe-Mo alloy was discussed. The extensive growth of columnar crystallites into the substrate provided excellent metallurgical bonding at the interface between the coating and the AISI 1045 steel substrate. The results showed that the microhardness and wear resistance of the coating were much higher than that of the AISI 1045 steel substrate. The lubricant MoO₃ formed in the transferred oxides layer also contributed to the wear resistance of the coating.

Keywords: plasma transferred arc cladding, Fe-Mo alloy coating, microstructure, wear resistance

Drilling in inconel 718 by femtosecond laser with burst mode

Xuan Liu^{1,2}, Wei Wang^{1,2}, Lijun Song^{1,2}

(1. State Key Laboratory of Advanced Design and Manufacturing for Vehicle Body, Hunan University;
2. Hunan Provincial Key Laboratory of Intelligent Laser Manufacturing, Hunan University)

liuxuanbdq@hnu.edu.cn

Abstract: In micro-holes drilling, the conventional manufacturing methods have its limitations. electrical discharge machining (EDM), for example, can only treat conductive materials; electrochemical holes drilling method has extremely low efficiency and limitation in material categories; mechanical drilling has difficulties in processing of high hardness materials and the aspect ratio of holes fabricated by mechanical method is relatively small. Compared to those traditional methods, femtosecond laser micro-hole processing has unique advantages, including wide material adaptability, non-contact fabrication, contamination free, high machining accuracy, etc. Though it has many distinctive advantages, there indeed are some shortcomings limiting its extensive application and development, as the method is poor efficient, time-consuming and has heat-affected zones when high frequencies pulses utilized. Researchers from Bilkent University showed that a burst of fs-laser that comprises of GHz pulse train could make ablation cooling possible, reduce the laser pulse energies needed for ablation and increase the efficiency of the removal process. It's believed that using of burst mode laser takes advantage of the heat accumulation effect to increase fabrication efficiency, and by properly controlling the parameters, the processing time will be shortened and the heat affected zone (HAZ) and recast layer would be reduced. Although there are a large number of documents focusing on the processing of micro-holes with the burst mode laser, there are few researches concerning fabrication of high aspect ratio holes on metals by burst. For that matter, we use burst mode lasers to fabricate holes on metals with different burst repetition frequencies, pulse widths, pulse energy and pulse number per burst contains and study their influence on hole quality. There are four processing types, which are single pulse drilling, percussion drilling, trepanning and helical drilling. We utilized helical drilling method to fabricate holes with a fixed pitch of 15 μm and diameter of 500 μm and chose various parameters to drill hole on an Inconel 718 alloy block. After the completion of the drilling processing, the metal block was sectioned using Wire EDM machine and polished with sandpaper, then cleaned in ultrasonic bath with ethanol to move debris. We applied a digital microscope to observe the upper surface and the shape of the holes. To determine the dimension of heat affected zone and recast layer, the samples etched by acid after polished and then observed with metallographic microscope to acquire the distribution of crystallites at the entrance of the hole. The results show that compared with conventional mode laser, the HAZ area and recast layer are similar when using burst mode laser. Besides, when power used in tow situations is same, the entrance of the hole fabricated by burst mode is much dirtier than the holes drilled by conventional mode, as there has more ablation deposition with more pulses in a burst. Another phenomenon is that with the increase of pulse number and keep the total energy of the burst remain unchanged, the depth and volume of the hole decrease gradually, and the bottom of the hole becomes rougher. When keep the energy of every single pulse in a burst remain unchanged and increase the pulse number in a burst, the depth and volume of hole increased, as the total energy deposited on sample increased.

Keywords: heat affected zone, ultrafast laser drilling, burst mode

Microstructure and corrosion resistance of FeCoCrNiCu high entropy alloying coating deposited by electro-spark process

Yanfang Wang
 (China University of Petroleum (East China))
 wang@upc.edu.cn

Abstract: High-entropy alloys (HEAs) have attracted extensive attention due to their unique structural properties. It is a hotspot in the coating field to produce HEA coatings by various surface treatments. In this paper, HEA coatings were prepared on 45Mn2 steel surface by electrospark deposition technique using FeCoCrNiCu0.5 and FeCoCrNiCu alloys as electrode. The phase compositions, microstructures and corrosion behaviors of the deposited coatings were analyzed by optical microscope (OM), X-ray diffraction (XRD), microhardness tester, and electrochemical measurement. The results show that both of the deposited coatings are dense and uniform with silver gray. The surface morphologies of the deposited coatings are orange peel-like and formed by deposition points superimposed to each other showing a typical “splash and sputter” and “crater” feature (Fig.1). The microstructures of the coatings both are FCC solid solution (Fig.2). The i_{corr} of the CrCoFeNiCu0.5 coating and CrCoFeNiCu coating is $7.319 \times 10^{-6} \text{ A/cm}^2$ and $5.249 \times 10^{-6} \text{ A/cm}^2$, respectively. Both of the coatings show excellent corrosion resistance with a higher E_{corr} and lower i_{corr} than 45Mn2 (Fig.3 and Fig.4).

Keywords: high-entropy alloy coating, electrospark deposition

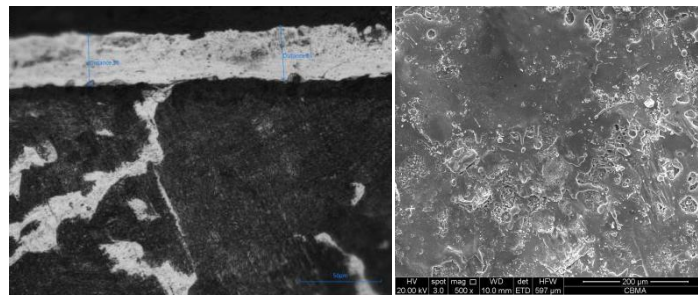


Fig.1 Microstructure of the deposited coating

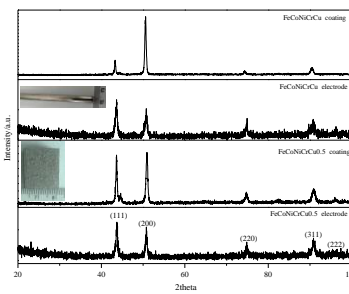


Fig.2

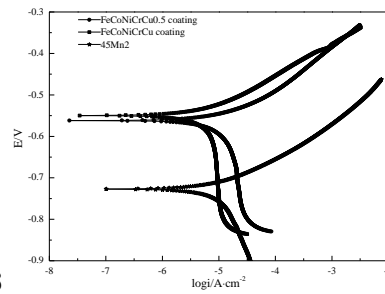


Fig.3

Fig.2 XRD of the deposited coatings and the electrode

Fig.3 Polarization curves of the deposited coatings and 45Mn₂ substrate in 3.5% NaCl solution

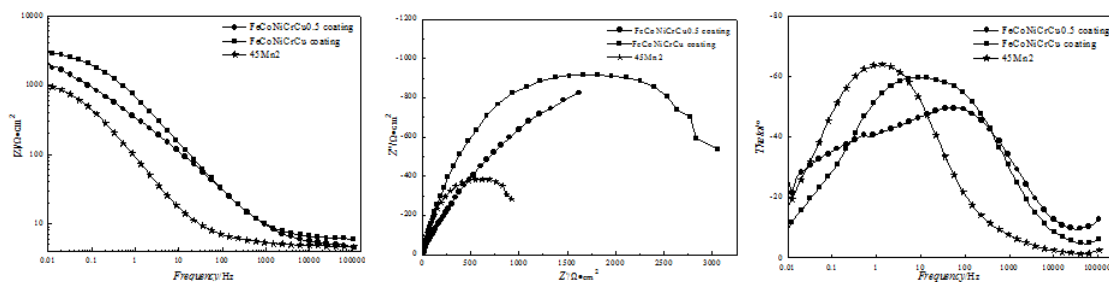


Fig.4 Electrochemical impedance spectroscopies of the deposited coatings and 45Mn₂ substrate

Comparative study on micro arc oxidation coatings on commercially forging and selective laser melting titanium alloy

Guolong Wu¹, Ye Wang¹, Min Sun¹, Qunli Zhang¹, Jianhua Yao¹, Volodymyr Kovalenko²
(1. Zhejiang University of Technology; 2. National Technical University of Ukraine)

laser@zjut.edu.cn

Abstract: Selective laser melting (SLM) is one of the latest additive manufacturing technology and has been used to fabricate titanium alloy biomedical implants. Like the traditional forging titanium alloys, the SLM titanium alloys also have poor biocompatibility and low wear resistance. Therefore, surface modification of SLM titanium alloys is very necessary. SLM titanium alloys generally have complex structures, and mechanical methods are difficult to achieve uniform surface treatment. Micro arc oxidation (MAO) is a promising technique based on electrochemical methods, and it can produce high hardness of ceramic layer on the surface of titanium alloy. During the MAO process, bioactive elements such as calcium and phosphate can be simultaneously incorporated into the coating from the electrolyte. Furthermore, MAO coating presents microporous structure which is very conducive to the improvement of biocompatibility. As an electrochemical surface treatment method, the growth of MAO coating is closely related to the microstructure and surface inhomogeneities of the substrate.

In order to better understand the influence of microstructure of titanium alloy with different manufacturing methods on the composition, surface morphology, properties of MAO coating in the same electrolyte, the growth process of Ca/P-based MAO coatings on forging-TC4 and SLM-TC4 parts was investigated and compared in this study. The microstructures, elements and phase compositions of MAO coatings on forging and SLM-TC4 were characterized by scanning electron microscopy (SEM), energy-dispersive spectroscopy (EDS), X-ray photoelectron spectroscopy (XPS) and X ray diffraction (XRD). Potentiodynamic polarization test was performed on the substrate and MAO coatings in simulated body fluid (SBF). The bioactivity of the coatings was carried out by immersion test in simulated body fluid (SBF). SLM-TC4 exhibit fine needles of α' phase, while forging-TC4 has distinct α and β phases. The experimental results show that the non-equilibrium phases of the SLMTC4 alloy make the discharge channels uniform and SLM-MAO coating is free of cracks. Although the MAO coatings on forging and SLM titanium alloy have almost the same growth rate in the early stage of MAO process, the typical porous characteristics of micro arc oxidation have appeared preferentially in SLM TC4. The thickness of SLM-MAO (SMAO) coating is slightly thicker than Forging-MAO (F-MAO) coating in the same condition. The amounts of Ca and P of S-MAO coating is higher than that of F-MAO. This is mainly due to the non-equilibrium phases of SLM-TC4 accelerate the micro-arc oxidation reaction to result in a thicker coating and higher amounts of Ca and P. S-MAO has a higher corrosion resistance and biological activity than that of F-MAO in SBF.

Keywords: selective laser melting, micro-arc oxidation, titanium alloy, selective laser melting, micro-arc oxidation, titanium alloy

Effects of cryogenic keeping time during cryogenic laser peening process on tensile properties and micro-structure of 2024-T351 aluminum alloy

Yunhui Sun, Jianzhong Zhou, Shu Huang, Jing Li, Yunjie Sun, Yangyang Xu
(School of Mechanical Engineering, Jiangsu University)

zhoujz@ujs.edu.cn

Abstract: Cryogenic laser peening (CLP) is a new strengthening technology which combines cryogenic treatment (CT) and laser peening (LP) to improve the comprehensive performance and stability of material by inducing severe plastic deformation, grain refinement and high density dislocation. This paper explores the mechanism of the coupling effect of ultra-high strain rate and ultra-low temperature on the surface integrity and tensile properties of 2024-T351 aviation aluminum alloy. The influence of different cryogenic keeping time on the tensile properties and microstructure of 2024-T351 aluminum alloy during the CLP process were investigated. The micro-hardness, residual stress and tensile properties of different 2024-T351 aluminum alloy samples were tested, and tensile fracture and microstructural evolution were observed by scanning electron microscopy (SEM) and transmission electron microscopy (TEM). The experimental results showed that the surface hardness increased with the prolongation of cryogenic keeping time. The surface hardness of CLP-0ed (CLPed of 0h cryogenic keeping time) and CLP-2ed (CLPed of 4 h cryogenic keeping time) samples reached 173.1 HV and 199.4 HV, and increased by 6.85% and 23.1% compared to LPed samples which of 162 HV, respectively. The highest residual compressive stress of CLP samples appeared at the near surface layer. Surface compressive stress of CLP-0ed and CLP-2ed samples reached 181 MPa and 223 MPa, compared with LPed samples of 163 MPa were increased by 11.04% and 36.8%, respectively. It indicated that prolongation of cryogenic keeping time could effectively eliminate the residual stress and enhance the effect of implanting of residual stress by cryogenic environment. Compared with untreated samples, the cryogenic treatment of 4 h keeping time can improve the strength and plasticity of the material at the same time. Compared with LPed samples, the tensile strength and elongation of CLP-0ed samples were increased by 5.2% and 10.7%, respectively, while for CLP-2ed samples were 13.2% and 26.8% respectively. For CLP-0ed sample, the internal defects of the material have not been consolidated and dissipated, and no enough residual compressive stress has been implanted. The prolongation of cryogenic keeping time could play a better reinforcement effect. In addition, CLP of 4 h cryogenic keeping time induced more grain-refinements and higher density dislocations. The depth of severe plastic deformation layer and slight plastic deformation layer induced by LP were about 250 μm and 450 μm , respectively, and the total depth of affecting layer was about 700 μm . Most of the grain size of the serious plastic deformation layer was below 50 μm , and the local grain is refined to less than 10 μm . Compared with the severe plastic deformation layer, the minor plastic deformation layer is coarser, and there is only local area grain refinement. However, most of the grains are still below 50 μm , while the original grain size of the matrix is mostly above 50 μm . Compared with the cross section of LPed samples, the severe plastic deformation layer and slight plastic deformation layer induced by CLP-2 were about 225 μm and 325 μm respectively, and the depth of the total affecting layer was about 550 μm . The investigations revealed that the strength and plasticity of the material were improved by the joint effect of grain refinement and dislocation strengthening, and the effect of cryogenic keeping time on 2024-T351 aluminum alloy in CLP process need to be further explored.

Keywords: cryogenic laser peening, 2024-T351 aluminum alloy, cryogenic keeping time, tensile properties, microstructures

Microstructure and mechanical properties of Fe901 fabricated by electromagnetic field-assisted laser additive manufacturing

Wenyuan He, Jianzhong Zhou, Jiale Xu, Shu Huang, Songtao Wang

(School of Mechanical Engineering, Jiangsu University)

hwynhm2012@163.com, zhoujz@ujs.edu.cn

Abstract: In order to improve the mechanical properties and overcome the defects of laser additive manufacturing (LAM) components, typical continuous fiber laser and a self-developed synchronous lateral powder feeding device were used to manufacture the iron-based (Fe901) coating under alternating magnetic fields. Vertical scanning and parallel scanning between layers were carried out during the process of LAM. The macroscopic morphology and microstructure evolution of the rectangular specimen prepared by two different scanning methods were compared and analyzed. Based on optimal LAM scanning path, the alternating magnetic field (AMF) was used during the LAM process. Comparison of the mechanical properties of the specimens fabricated by alternating magnetic field-assisted and the standard annealed forgings (SAFs), the effects of the alternating magnetic field on the microhardness, phase composition and wear resistance of LAM specimens were investigated. The cross-sectional microstructure of the samples were analyzed by optical microscope (OM) and scanning electron microscope (SEM). The phase composition were investigated by X-ray diffractometer (XRD). The microhardness were measured with a FM-700 microhardness tester. Meanwhile, the wear and friction test of the samples with and without AMF and the SAFs were conducted at 150 N with the friction pair of Si₃Ni₄ ceramic ball, thereby the corresponding wear mechanisms were discussed. The results showed that the samples with good shape profile, smooth surface, obviously refined grains, free of micro-cracks and porosity when the intensity of the electromagnetic field above the molten pool is in the range of 30-40 mT. The microhardness of the sample produced by electromagnetic field-assisted laser additive manufacturing is about 675.8 HV0.2 which is about 1.8 times higher than that of the sample without AMF. However, the microhardness of the electromagnetic field-assisted LAM specimen is 0.89 times of the SAFs, which is very close to the mechanical properties of SAFs one. The phase composition of the samples with and without AMF were composed of α -(Fe, Cr), (Cr, Fe)₇C₃, CrFeB, FeCrMo, and there was no a new phase formed. The coefficient of friction of the samples with and without AMF and the SAFs one were 0.543, 0.645 and 0.508 respectively. The wear resistance of the sample with AMF was significantly higher than that of the sample without AMF, and the amount of wear mass loss in the friction and wear test was 0.4 times of the one without applied AMF. However, the height of the sample with AMF under the same process parameters is reduced, which reduced the forming efficiency. It was concluded that the application of AMF resulted in the refinement of microstructure and transformation from the columnar dendrites to a fine equiaxed crystal structure in the LAM process. And also it can reduce the metallurgical defects and improve the surface quality as well as increase the microhardness and wear resistance of the sample which fabricated by LAM assisted by AMF.

Keywords: laser additive manufacturing (LAM), electromagnetic field, microstructure, mechanical properties

Study on mechanical properties and microstructure of laser cladded graphene nano-platelets reinforced Inconel 625 superalloy composite coating

Pingshun Deng, Kai Feng, Zhuguo Li
(Shanghai Jiao Tong University)
fengkai@sjtu.edu.cn

Abstract: Laser cladding is an advanced and high-efficient surface modification technology to deposit a hard layer with controlled thickness on the selected area of a metal substrate. Mainly because of its superior characteristics, such as high power density, rapid cooling velocity as well as small heat-affect zone (HAZ) in the base material, this technique has wide applications in aviation, marine and turbine industries and so on. In recent years, laser cladded Inconel 625 (IN625) have a wide application in turbine engines, chemical, marine and nuclear industries because of its superior wear, corrosion and oxidation resistance. Associated with the new concept of metal matrix composite (MMC) which combines its metallic properties with ceramic properties to display greater resistance to aggressive environment, higher hardness, advanced mechanical strength and improved wear properties were continuously founded beyond the pure material. However, the carbon nano-fiber-based reinforcement in laser cladding has been seldom studied because the fiber structure is vulnerable in highly intensive laser beam. In this study, a protective coating was designed surrounded the carbon materials to prevent from damage during the laser cladding process. Specifically, an innovative and simplified method of electroless pure-nickel coating was stably and evenly plated on graphene nano-platelets (GNPs). The nickel-coated graphene nano-platelets (NiGNPs) were uniformly dispersed in Inconel 625 (IN625) powder with the ratio of 1:9 by ball milling. Then laser cladding was used to fabricate the NiGNPs reinforced IN625 composite coating, GNPs added IN625 and pure IN625. The survivability of GNPs, morphology of precipitated phase, microhardness through transverse section, wear resistance at room and elevated temperatures and mechanical properties were studied. The results indicated that the NiGNPs were successfully incorporated into IN625 coatings by laser cladding. Part of them were deduced to be damaged or dissolved into molten pool, which benefited the formation of NbC, but most of them could be observed as exposed GNPs and well-distributed welded GNPs. Whereas without protective coating, less GNPs and more chromium carbide can be founded in the GNPs reinforced laser cladded samples because naked GNPs can be easily dissolved in the molten pool and enhanced the formation of carbides. Compared to laser cladded IN625 coating, the composite coating showed higher hardness at bottom region of cladded coating and smaller size of HAZ due to the improvement of thermal conductivity by additional NiGNPs. Comparative wear test demonstrated that friction coefficient (COF) and wear rate were decreased at both room and elevated temperatures. Combined with wrinkled, tiled and rolled GNPs observed on the worn surface, it was revealed that the wear properties were efficiently benefited from superior lubrication between interlayers of GNPs. Furthermore, the GNPs reinforced composite coating exhibited highest yield strength up to 593 MPa, but the elongation was seriously decreased down to 12%. Whereas, the NiGNPs samples, with lower yield strength, demonstrated around two times of elongation which benefited from the protective coating on GNPs. Thus, GNPs could survive and act as reinforced in laser cladding process under protective coating, which effectively enhance the hardness, wear resistance and yield strength of IN625.

Keywords: laser cladding, inconel 625, carbon nano-platelets, hardness, tensile strength, wear resistance

Effects of Ni/Co on properties of aluminum bronze laser claddings

Xiangxiang Huang, Zhuguo Li

(Shanghai Key Laboratory of Materials Laser Processing and Modification)

lizg@sjtu.edu.cn

Abstract: Aluminum bronze (AB) is one kind of copper alloy widely used in marine environment, for example valves, tubes and propellers, due to its excellent corrosion resistance and good strength. Low carbon steels have been mass-produced and used on ships as structural steels due to their low cost and good weldability and strength, for example the fastening pieces. However, carbon steels have poorer performance than copper alloy at resisting water corrosion. In order to repair and improve the surface properties of low carbon steel, aluminum bronze can be cladded on them to offset the deficiency.

The AB powder was surfaced on low carbon steel plates by high power diode laser with laser power 4 kW, scanning speed 2 mm/s and power feeding rate 10.064 g/min. The chemical composite of AB powder is (wt%): 81.16%Cu, 7.87%Al, 5.08%Fe, 5.50%C, 0.39%Mn. Then 5%Ni and (5%Ni, 5%Co) were added into AB powder by ball-milling respectively to research on the microstructure and properties difference.

To observe the transverse microstructures, an optical microscope and a scanning electron microscope equipped with an energy dispersive X-ray spectroscopy system were used. XRD spectra of cladding was observed by X-ray diffraction analyzer, with incident angle (2θ) ranging from 20° - 100° .

To investigate the properties of AB alloy claddings, Vickers hardness was tested on the cross-section of cladding, with 300 g loading for 15 s. To simulate the sea-water environment, electrochemical corrosion test was carried out in 3.5% NaCl solution. The potential scanning rate is 0.5 mV/s from -1.0 V to 0.2 V.

The typical microstructure of AB cladding contains Fe-rich phases and Cu-rich phases due to liquid separation. Ni distributes uniformly and changed the microstructure of AB cladding to some extent. The Fe-rich phases turn from irregularly-shapes into globular shapes, also the size of Fe-rich phase is much smaller. However, Co allocates mainly in the Fe-rich phases and reduced the formation of Fe-rich phase. Co exists in the form of α -Co and CoC_x .

The average microhardness of AB cladding is 225 HV, while that of AB (5%Ni) and AB (5%Ni, 5%Co) cladding are 237 HV and 244 respectively.

Three electrochemical polarization curves are very similar in 3.5% NaCl solution. When potential goes beyond about -0.3 V, the current reaches a peak, then slowly decreases, which indicates a passive film forming at the surface. After Tafel calculation, it is clear to see that the corrosion potential of AB (5%Ni) and AB (5%Ni, 5%Co) cladding are higher than that of AB cladding. But the current density of AB (5%Ni) cladding is larger than AB cladding while that of AB (5%Ni, 5%Co) is lower than AB cladding.

1) Three claddings all undergo primary liquid separation, but only AB and AB (5%Ni) claddings can observe secondary liquid separation, while AB (5%Ni, 5%Co) cladding does not have this phenomenon.

2) 5%Ni addition increases the microhardness of AB cladding, but slightly increases the corrosion rate due to finer microstructure.

3) (5%Ni, 5%Co) addition obtains the best properties among three claddings due to the distribution of α -Co.

Keywords: aluminum bronze, laser cladding, Ni/Co, microstructure, properties

Selective laser melting of Ti-Mo based alloys

Qiaochu Li, Xiaohua Min, Tianyu Liu, Qun Yu, Cunshan Wang, Chuang Dong
(School of Materials Science and Engineering, Dalian University of Technology)
minxiaohua@dlut.edu.cn

Abstract: β -type Ti-Mo alloys have high specific strength, low elastic modulus and good corrosion resistance, which make them an attractive choice of many fields as functional materials and structural materials. The characteristics of these alloys are the variety in phase transformation and deformation mode which are a function of β phase stability. These phase transformation is also an advantage in biomedical fields, such as changeable modulus. Design and manufacture of complex shape Ti parts with good quality are highly demanded in biomedical areas. Selective laser manufacturing (SLM) is an additive manufacturing process in which complex parts were produced by selectively melting consecutive layers of powder with a laser beam. Existing Ti-Mo alloys haven't show excellent performance in additive manufacturing compared with traditional Ti-6Al-4V alloy. There is still a lack of systematic analysis to improve mechanical behavior of Ti-Mo alloys by additive manufacturing. In order to find proper Ti-Mo based alloy components suitable for additive manufacturing, "Cluster-plus-Glue-Atom" Model was used in this study to design alloy components. "Cluster-plus-Glue-Atom" Model which based on the short-range-order between atoms in solid solution alloy can give a good picture of interaction of each element. Materials suitable for 3D printing must have good melt stability and high compatibility between melt and solid structure. These characteristics are narrow in solid-liquid phase in phase diagram, and congruent points on some alloy phase diagrams. Congruent point can be explained by "Cluster-plus-Glue-Atom" Model. Ti-Mo binary phase diagram had no congruent point. Addition of other elements may improve the mechanical behavior of Ti-Mo alloy manufactured by selectively laser melting. After a lot of calculation with different elements used in Ti alloys, Ti-13Mo-8Zr-2Fe-1Al, Ti-11Mo-10Zr-2Fe-2Al, Ti-13Mo-8Nb-2Fe-1Al and Ti-11Mo-10Nb-2Fe-2Al were selected in this study. Ti-15Mo and Ti-6Al-4V were prepared as contrastive materials. Each kind of alloy were build up into cube for mechanical behavior tests by selective laser melting. Mechanical behavior and microstructure characterization were examined systematically. The pure metal powder with a nominal particle size distribution between 50 and 150 μm were used in this study. 2 hours powder mix were for each alloy. Selective laser melting was performed on a Dalu laser machine. For microstructural observations, samples were subjected to mechanical-chemical polishing to obtain a smooth surface with SiC waterproof emery paper up to 320 grit, followed by polish with polycrystalline diamond suspension of 9 μm and 3 μm , respectively, finally polished with a mixture solution of SiO_2 and H_2O_2 . The mirror-polished specimens were etched for 20 s with a solution of distilled water, nitric acid and hydrofluoric acid (100:3:2 by volume). Microstructures were observed by MEF4A optical microscopy. Samples for Vickers hardness test were polished and then were measured with a load of 9.8 N for 15 s (HVZ1000S) at fifteen points from edge to center position, with their average taken as the value for that sample. Compressive tests also carried out to compare the mechanical behavior of each sample. After addition of other elements, surface of Ti-Mo based alloy Ti-Mo based alloys designed by "Cluster-plus-Glue-Atom" Model show excellent mechanical behavior compared with traditional Ti-6Al-4V alloy and Ti-15Mo alloy.

Keywords: Ti-Mo alloy, additive manufacturing, "Cluster-plus-Glue-Atom" model

Microstructure evolution and wear behavior of in-situ synthesis boride and carbide particle reinforced Ni60CuMoW coating by combination of laser cladding and tempering treatment process

Hongxi Liu

(Kunming University of Science and Technology)

piiliuhx@sina.com

Abstract: Carbide and boride ceramic particle reinforced Ni60CuMoW composite coatings were fabricated by combination of laser cladding in-situ synthesis and tempering treatment process on 45 medium carbon steel. The chemical composition, reinforcement distribution and microstructure evolution of composite coatings were investigated by optical microscopy (OM), X-ray diffraction (XRD), scanning electron microscopy (SEM) and energy disperse spectroscopy (EDS). The influence of tempering treatment on microstructure and wear mechanism of composite coating was analyzed. XRD and EDS results showed that the composite coating mainly consisted of γ (Ni, Fe), (Ni, Cu) solid solution, Ni₃₁Si₁₂ intermetallic compound, CrB boride and M₂₃C₆ type carbide particle reinforced phases. The particle reinforced phases in composite coating after tempering showed a uniform and dense morphology and a good metallurgical bonding with substrate in 0.3-0.8 mm thickness range. Compared with substrate, the average hardness of laser cladding composite coatings without and with tempering treatment increased by 4.9 times and 5.8 times, and the relative wear resistance increased by 1.1 times and 2.9 times, respectively. The worn surface of composite coating without tempering shows an apparent furrow-like and belongs to surface fatigue wear mechanism. But for the composite coating after tempering, the wear surface is relatively smooth and shows a shallow scratch, good adhesion and small size of wear debris, belongs to abrasive wear mechanism. The tempering treatment can promote the formation of particle reinforced phases, improve the microstructure compactness in laser cladding composite coating, and make the cladding coating not easy separate from the substrate in wear process.

Keywords: laser cladding, composite coating, tempering treatment, microstructure evolution, wear behavior

Investigation on wear resistance of nodular cast iron by laser heat treatment

Hongyin Zhu, Wenfu Cui, Yan Shi, Jia Liu

(Changchun University of Science and Technology)

liujia@cust.edu.cn

Abstract: The surface of nodular cast iron is treated by laser melting and quenching with 5 kW CO₂ laser in order to study the impact of two methods on the material wear resistance. The results show that the material vickers-hardness after laser heat treatment is significantly improved, and the hardness of the area treated by the laser melting is slightly higher than that of the laser quenching treatment. The analysis of friction and wear test shows that the wear resistance of the area after heat treatment obviously improves compared with the substrate's and the laser quenching has more obvious influence on the wear resistance than the laser melting. On the one hand, the material hardness after heat treatment is clearly higher than that of the substrate, which makes wear resistance of the material greatly improved. On the other hand, laser quenching has little effect on graphite in nodular cast iron. The retained graphite has a lubrication action, which reduces the friction coefficient and improves the wear resistance.

Keywords: nodular cast iron, laser melting, laser quenching, hardness, wear resistance

Influence of metal coating on laser welding of glass

Hao Wang, Qingmao Zhang, Liang Guo, Xin Zhang
(South China Normal University)
Zhangqm@scnu.edu.cn

Abstract: Glasses are widely used in our life, but the traditional glass sealing methods have a lot of restrictions on the sealing condition and using environment. Different from the traditional sealing method, laser welding can control the welding area accurately, and it has little influence on the mechanical properties of glass. The present researches are mainly focused on the ultra short (US) pulse lasers welding. Its mechanism is the nonlinear absorption of ultra short pulse laser by glass, and it causes cracks in glass. So it significantly affects the transparency of glass. In comparison with the metal coating as the solder, the joined glasses which had almost no damage could be obtained. The influence on optical and mechanical properties was greatly reduced. And the metal coating improved the laser absorption efficiency of the samples, so that the nano-second laser could complete the welding. At this work, 1mm thickness glasses coated with 50-1000 μm metal by physical vapor deposition (PVD). Then through the irradiation with a nano-second pulsed Nd:YAG laser (wavelength, 1064 nm). Samples with little damage were obtained in suitable laser parameters. The laser absorptivity of sample increased with the increasing of film thickness. When coated with 50-150 nm titanium, the irradiated sample showed high transmittance.

Keywords: laser welding, nano-second pulsed laser, metal coating, glass

Effect of dislocation behaviors on micro-structural evolution of laser shock processed commercial pure aluminum and aluminum alloy 2A02

Xinmin Luo
(Jiangsu University)
791197039@qq.com

Abstract: The relations between dislocation behavior and microstructural evolution of commercial pure aluminum and aluminum alloy 2A02-T6 by laser shock process (LSP) were investigated. Specimen hardness curves in the laser-shocked surface region were measured. Microstructural features of the hardened layer and comparison between α -aluminum and the aged aluminum alloy were characterized by transmission electron microscopy (TEM) and inverse fast fourier transform (IFFT). It was found that the multiplication and motion of dislocations could remarkably influence the microstructural evolution of the test materials upon multiple LSP. A large number of dislocations induced in commercial pure α -aluminum upon LSP coupled with the increased deformation and then became waved and net-shaped which finally produced dislocation tangles (DTs) and dislocation cells (DCs). The dislocation density was closest near grain boundaries. The semi-coherent relationship between precipitates and the matrix of the aluminum alloy 2A02-T6 and manifestation of nanocrystalline behavior were both observed in the LSP zone. The grain size in the hardened surface by LSP was about 100 nm. The nanocrystallization process after multiple LSP can be summarized as follows: 1) formation of dislocation-induced LSP in original grains; 2) dislocation multiplication; 3) formation of dislocation walls (DWs) due to a geometrically necessary dislocations (GNDs) effect; 4) formation of subgrains; and 5) nanocrystallization. DTs and DCs, DWs and nanocrystallization become the main physical metallurgy behaviors upon LSP for commercial pure aluminum and aluminum alloy 2A02-T6 respectively.

Keywords: laser shock process, dislocation

Investigation on the microstructure and properties of different nickel-based coatings deposited by laser cladding

Meiyan Li, Qi Zhang, Han Bin
(China University of Petroleum)
limeiyan@upc.edu.cn

Abstract: Surface coating technology is an important method in the surface engineering fields, which could improve the microstructure and properties of the machine parts. Laser cladding has advantages of energy concentration, small heat affected zone, low dilution rate, high strength metallurgical bonding between the coating and matrix and so on. In this paper, different Ni-based coatings were prepared by laser cladding and the microstructures, phase composition and properties were compared and analyzed by means of scanning electron microscopy (SEM), X-ray diffraction (XRD), transmission electron microscope (TEM), hardness tester and friction abrasion testing machine. The microhardness of Ni-20% WC coating is high than that of the matrix, but fluctuates greatly. The addition of 316L powder leads to the decrease of microhardness while the continuous addition of 5%Cr₃C₂ powder results in higher hardness and uniform distribution. In addition, the weight loss of the Ni-20%WC+30%316L+5%Cr₃C₂ coating is lowest compared with the other two Ni-based coatings, about half of the Ni-20% WC coating, which indicates the best wear resistance.

Keywords: laser cladding, Ni-based coating, ceramic phase, microstructure, property

Microstructure and corrosion behavior of amorphous Ni-Cr-Si-B-Fe coating fabricated by laser additive manufacturing

Zexin Chang¹, Wenxian Wang¹, Yaqiong Ge²
(1. Taiyuan University of Technology; 2. Taiyuan University of Science and Technology)
wangwenxian@tyut.edu.cn

Abstract: In this study, focus will be on producing an amorphous coating on mild steel through laser additive manufacturing of an amorphous Ni-Cr-Si-B-Fe ribbon instead of powders. This study aims to test the feasibility and understand the fundamentals of using a sustainable and low-cost ribbon rather than the customized powders to fabricate an amorphous coating using laser additive manufacturing method. Ni-Cr-Si-B-Fe amorphous ribbon was successfully coated on a mild steel substrate by laser additive manufacturing. The microstructure, phase composition, chemical component distribution, and corrosion behavior of the coating were systematically investigated. The results of X-ray diffraction showed that amorphous and crystalline phases coexisted in the coating. According to SEM and TEM analyses, middle and surface regions of the coating were mainly consisted of eutectic structures. Columnar crystals existed in the bottom region of the coating near the coating-substrate interface. The matrix of the coating was mainly consisted of amorphous phase and the γ (Fe, Ni) solid solution phase. The coating exhibited excellent corrosion resistance. Due to more rapid cooling in the surface region of the coating, more amorphous phases formed there and material there demonstrated better corrosion resistance than that in the middle region of the coating. The corrosion resistance of the coating was found to be improved with increasing amorphous phase content in the coating.

Keywords: amorphous ribbon, laser additive manufacturing

Stress and temperature distribution for arc weld-based rapid prototyping of titanium alloy TC4

Xizhang Chen¹, Huili Xu², Guifang Xu²
(1. Wenzhou University; 2. Jiangsu University)
chenxizhang@wzu.edu.cn

Abstract: Weld-based rapid prototyping is an inexpensive manufacturing technology developing on the layered manufacturing to shape metal parts along stated paths. In this paper, the thermal and stress distributions in a single-pass multi-layer weld-based rapid prototyping for the titanium alloy TC4 were examined by numerical simulation. The results showed that peak values of a single thermal cycle in a deposited layer gradually decreased as the increase of the deposited layers. The accumulation of heat was obvious by comparative analysis of peak values of different deposited layers in the same thermal cycle. The peak temperature of the last deposited layers increased at first and then tended to stabilize as the increase of the deposited layers due to the accumulation of heat. Besides, preheating treatment effectively reduced the interior stress of the deposited part making the stress distribution uniform. The rear layer had a re-melting or post-heating effect on the front layer relaxing the stress of the stacking part to a certain extent.

Keywords: stress, simulation, wire arc based additive manufacturing

Influences of inclination angles on microstructure and mechanical properties of 316L stainless steel parts fabricated by selective laser melting (SLM)

Cong Ni, Yan Shi, Jia Liu
(Changchun University of Science and Technology)
lasercust@hotmail.com

Abstract: Selective laser melting (SLM) is the main kind of additive manufacturing methods that fabricated complex functional components based on local melting of a metal powder bed by a using a high-energy laser beam. In this work, the SLM process was used with various inclination angles to fabricate samples. The correlation between the inclination angles, the densification behavior, the residual stress, the obtained microstructure and the mechanical properties was investigated. Results indicated that when the inclination angle was 0°, it owned the better mechanical properties and the densification behavior. The residual stress of 0° was larger than others and the 45° was the minimum. The major type of tensile fracture was ductile fracture, while 90° was fragile fracture because of imperfections.

Keywords: selective laser melting, inclination angles, mechanical properties, imperfection

Influence of O₂/N₂ flow ratio on the microstructure and properties of AlCrON coatings deposited by multi-arc ion plating

Ahmad Farooq^{1,2}, Qing Liu^{1,2}, Lin Zhang¹, Qimin Wang^{1,3}, Shihong Zhang^{1,2}

(1. Research Center of Modern Surface & Interface Engineering, Anhui University of Technology, China;

2. School of Materials Science and Engineering, Anhui University of Technology, China;

3. School of Electromechanical Engineering, Guangdong University of Technology, China)

tougaoyouxiang206@163.com

Abstract: In the present work six groups of coatings with 0-40% O₂/N₂ flow ratio were deposited on plasma nitriding H13 steel substrates by multi-arc ion plating with 5 μm thickness. The influences of O₂/N₂ flow ratio on composition, microstructure, and mechanical properties, as well as the tribological properties, of the coatings were investigated. With increasing oxygen content, the coating microstructure gradually evolves from single fcc-(Cr, Al)N phase to the mixture of AlN, CrN and (Cr, Al)ON solid solution which corresponds to an increased crystallinity within the coatings. The coating presents the highest hardness and best roughness at lower O₂ flow ratio of 10at%, but the coating adhesive strength and inner stress increase with increasing oxygen flow ratio. The incorporation of oxygen in the nitride structure and the incorporation of the nitrogen atoms in the oxide structure in combination with the transition region between the oxide and nitride structure can be considered responsible for the favorable mechanical properties and thermal stability of the oxy-nitride coatings.

Keywords: plasma nitriding, AlCrON coating, coating structure, properties

Design of Fe-alloy/Ni-alloy multi-layered laser cladding coatings for repairing and remanufacturing GCr15 rollers

Ting Liu^{1,2}, Yi Zhao^{1,2}, Lin Zhang¹, Shihong Zhang^{1,2}, Mingxi Li²

(1. Research Center of Modern Surface & Interface Engineering, Anhui University of Technology, China;

2. School of Materials Science and Engineering, Anhui University of Technology, China)

tougaoyouxiang206@163.com

Abstract: Multi-layered coatings of Ni-based alloy were successfully cladded onto GCr15 hardened steel substrates for remanufacturing by a fiber laser and synchronous powder feeding system. The effects of laser power and scanning speed on the microstructure and mechanical properties of the cladding layer were investigated. The microstructure of the coating was investigated by means of metalloscopy, X-ray diffraction and scanning electronic microscopy. The surface and cross-section hardness, impact toughness, wear resistance and corrosion resistance of the coatings were measured. The thickness of laser cladding coating is about 5 mm. The different laser power and scanning speed used in the experiment had influence on the structure size of the cladding layer and element distribution. The laser cladding coating is metallurgical bonding with the substrate and the microstructure is fine without cracks and voids. The coatings exhibited a gradient distribution in cross-section hardness and surface hardness of about 59 HRC. The coating exhibited good impact toughness, wear resistance and excellent corrosion resistance.

Keywords: laser cladding, nickel-based alloy, microstructure, wear performance

Study on structures and properties of laser surface alloying of

Co-based alloyed layer on ductile iron hot roller

Yi Zhao^{1,2}, Fei Cai¹, Shihong Zhang^{1,2}

(1. Research Center of Modern Surface & Interface Engineering, AHUT, China;

2. School of Materials Science and Engineering, AHUT, Maanshan 243002, China)

tougaoyouxiang206@163.com, shzhang@ahut.edu.cn

Abstract: Laser surface strengthening technology has been widely used in recent years. In this paper, cast iron was used as the base material and Co alloy powder used as alloying material. Effects of laser scanning speeds on the microstructure, microhardness, wear resistance and thermal fatigue of laser alloyed layer were investigated by X-ray diffractometer (XRD), Scanning electron microscopy (SEM), micro-hardness tester, high temperature wear apparatus. The results show that thickness of alloyed layer was between 0.31 mm and 0.36 mm, and the hardness of alloyed layer was about 3-4 times higher than that of matrix. Moreover, in a certain range, the hardness increased first and then decreased with the increase of scanning speed. The crack rate increased with the increase of scanning speed. The experimental results of wear showed that wear resistance of alloyed layer at 400 °C increased with the increase of scanning speed. The wear mechanisms of alloying layer were adhesive wear, abrasive wear and oxidation wear.

Keywords: ductile iron hot roll, laser surface alloying, hardness, wear resistance, crack rate

Study on corrosion and corrosive wear behaviors of N-doped Ni-Cr coatings deposited by arc ion plating

Ying Yang¹, Yedong Wu^{1,2}, Le Li^{1,2}, Lin Zhang¹, Fei Cai¹, Shihong Zhang^{1,2}

(1. Research Center of Modern Surface & Interface Engineering, Anhui University of Technology, China;

2. School of Materials Science and Engineering, Anhui University of Technology, China)

tougaoyouxiang206@163.com, shzhang@ahut.edu.cn

Abstract: In this study, N-doped Ni-Cr coatings were fabricated on 42CrMo substrates by means of arc ion plating in Ar-N₂ atmosphere. Different nitrogen flow rates (0-600 sccm) were introduced to tailor the coating N contents. The X-ray diffraction patterns illustrated that all N-doped Ni-Cr coatings were composed of (Cr, Ni)N and (Ni, Cr) solid solution independent of nitrogen flow rates. The coating microhardness increased with an increase in nitrogen flow rates, while the adhesion strength almost kept the same (HF1-HF2). Electrochemical potentiodynamic polarization results demonstrated that all coatings exhibited more positive E_{corr} and much smaller i_{corr} compared to the substrate, indicating excellent corrosion resistance of the coatings. The corrosive wear resistance of N-doped Ni-Cr coatings was better than that of Ni-Cr coating due to the higher microhardness of (Cr, Ni)N ceramic phase in the former coatings. When the nitrogen flow rate was 200 sccm, the coating exhibited best corrosive wear resistance. With further increasing nitrogen flow rates, the corrosive wear resistance decreased as a result of less amount of metallic phase, which deteriorated the pitting corrosion resistance of the coatings. The mechanism of corrosive wear resistance were also discussed in detail in this paper.

Keywords: Ni-Cr coatings, N-doped, corrosive wear resistance, arc ion plating

Corrosive wear properties of Cr₃C₂-NiCr-TiN/TiAlN duplex coatings

prepared by combination of HVOF and arc ion plating

Kai Hu^{1,2}, Xiangjun Cheng^{1,2}, Xia Liu¹, Lin Zhang¹, ShihongZhang^{1,2}

(1. Research Center of Modern Surface and Interface Engineering, Anhui University of Technology, China;

2. School of Materials Science and Engineering, Anhui University of Technology, China)

tougaoyouxiang206@163.com

Abstract: The duplex coating Cr₃C₂-NiCr-TiN/TiAlN was successfully prepared on the surface of carbon steel substrates by combination of high velocity oxygen-fuel (HVOF) and multi-arc ion plating (PVD). The corrosive wear behavior of sprayed Cr₃C₂-NiCr coating, TiN/TiAlN bilayer coating and duplex composite coating were investigated by wet pin-on-disk wear experiments immersed in corrosive environments consisting of sodium chloride solution with the chloride ions concentrations of 5, 10 and 15 vol%. The electrochemical corrosion studies were carried out by using potentiodynamic polarization curves and electrochemical impedance spectroscopy (EIS) in comparison with steel substrate in 3.5 wt% sodium chloride solution. The results showed that the increase of the chloride ions concentration considerably deteriorated the wear resistance of the coated samples. The wear resistance of the duplex coating is better than that of a single spray coating, and the PVD bilayer coating could effectively prevent the expansion of chloride pitting corrosion. Compared with the sprayed Cr₃C₂-NiCr coating, duplex coating showed more stronger corrosion resistance, and the impedance of the composite coating increases faster than that of the sprayed coating. The hardness of the Cr₃C₂-NiCr coating was greater than steel substrate, which was contributed to increase the carrying capacity, and obviously improve the overall performance of the duplex coating.

Keywords: HVOF, PVD, corrosive wear, electrochemical corrosion

Microstructure and mechanical properties of SA336F12 fabricated by electricity melting additive manufacturing technology

Chenggang Zhi, Lianju Yan, Yan Zuo

(NanFang Additive Manufacturing Technology Co., Ltd.)

Abstract: The ring-like sample of the LAHS SA336F12 which is applied to the mechanical piping penetration of the new generation nuclear power was fabricated by electricity melting additive manufacturing technology. The testing results showed that the specimens is characterized by macro feature of columnar crystal, microstructure character of acicular ferrite microstructure sub-grains and excellent mechanical properties at room temperature. The circumferential, axial and radial tensile strength of the test piece reached 595, 595 and 585 MPa, and elongations 28%, 29% and 30% respectively, and no obvious directivity. The microstructure characteristics of the sample is determined by the process characteristics of additive manufacturing technology, and the excellent mechanical properties showed that this technology is easy to achieve the strengthening and toughening of the low carbon and low alloy structural steel.

Keywords: microstructure, mechanical properties, electricity melting

Mechanical properties and corrosion behaviors of TiN/TiAlN multilayer coatings by ion source enhanced hybrid arc ion plating

Gui Li^{1,2}, Wen Huang^{1,2}, Lin Zhang¹, Shihong Zhang^{1,2}

(1. Research Center of Modern Surface & Interface Engineering, Anhui University of Technology, China;

2. School of Materials Science and Engineering, Anhui University of Technology, China)

tougaoyouxiang206@163.com, shzhang@ahut.edu.cn

Abstract: TiN/TiAlN multilayer coatings with different bilayer cycles (2, 4, 6, and 12) were successfully deposited on martensite stainless steel (MSS) using ion source enhanced hybrid arc ion plating technique. The microstructure, cross sectional and surface morphologies, wear performance and corrosion behaviors of multilayer coatings were investigated systematically by means of XRD, SEM, step profile, microhardness tester, ball-on-disk tribometer, electrochemical measure in 3.5% NaCl solution, respectively. XRD results revealed that the as-deposited coatings were mainly composed of FCC-TiN and (Ti, Al)N phases with (111) preferential orientation, and the growth tendency of preferential orientation was abated with the increase of bilayer cycles. All coatings exhibited excellent adhesion strength. The microhardness of coatings increased with the increase of bilayer cycles, reaching a maximum of 3800 HK_{0.025} at the 12 bilayer cycles. The tribological performance indicated that the abrasive wear and oxidation wear were the dominant wear modes for multilayer coatings under WC pair. The lowest friction was obtained at the 12 bilayer cycles, and the bilayer cycles have no significant influence on the wear properties of as-deposited coatings. Electrochemical results exhibited that the multilayer coatings improved obviously the corrosion resistance of the MSS substrate. In addition, the corrosion resistances of these coatings and the bilayer cycles were not accorded with the linear relationship exclusively.

Keywords: TiN/TiAlN multilayer coatings, structure, mechanical properties, corrosion behaviors

The methodology research of industrial design for remanufacture

Wanxuan Yuan

(The Department of Mechanical Engineering, Guangdong Polytechnic of
Water Resources and Electric Engineering)

yuanwx@gdsdxy.cn

Abstract: Under the trend of low carbon manufacturing and green design, remanufacture is reasonable choice and actual existence. Industrial design as the source of all kinds of products, should concern about the remanufacture that will benefits product developing, prolong the product life and cuts down the cost of products. This paper, introduced the utilization of remanufacture in product developing, concluded some key factors to utilizing and considering of remanufacture, enumerated some benefits of considering remanufacture in industrial design, proposed some methods of considering remanufacture during industrial design, brought out some prospects of remanufacturer's utilization in the field of industrial design.

Keywords: methodology research, industrial design, remanufacture

Microstructure and tensile properties of laser additive repaired titanium alloy

Zhuang Zhao, Jing Chen, Fenggang Liu, Hua Tan, Weidong Huang

(State Key Laboratory of Solidification Processing, Northwestern Polytechnical University)

Abstract: The microstructure and tensile properties of laser additive repaired (surface repair) TC4 titanium alloy were investigated in this paper. The macrostructure of the repaired specimen can be divided into three domains: laser deposited zone (LDZ), heat affected zone (HAZ) and wrought substrate zone (SZ). The room temperature tensile test show that the strength and ductility of the wrought specimen are slightly higher than that of the repaired specimens. Meanwhile, the strength of the repaired specimen with repair ratio of 40% is slightly lower than that of 50% repaired specimen, but the ductility is higher than the latter. The wrought specimen tensile fracture presents a typical ductile characteristic, and the repaired specimen shows a complex fractograph. From the SZ to the LDZ, the tensile fracture presents a successive transformation from dimple fracture to cleavage step. It can be seen that there is a good corresponding relationship between the fracture morphology and the microstructure of the repaired specimens.

Keywords: microstructure, tensile properties, laser additive repaired titanium alloy

Effect of annealing on the microstructure properties of supersaturated

Cu-Cr alloy film and bulk

Xiaoxue Huang, Yechang Chao, Haoliang Sun, Guangxin Wang

(Henan University of Science & Technology, Luoyang, Henan, China)

Abstract: With the rapid development of flexible display and smart wear technology, it is urgent to carry out the design and development of high performance nano-film materials on flexible substrate. Copper (Cu) thin films and bulk alloy have been widely applied in the field of microelectronic devices, solar cells and so on due to their excellent electrical and thermal conductivity, corrosion resistance and mechanical properties. As the size of the film is gradually reduced to the nano-sized, the effect of the external field on the microstructure of the film material becomes more obviously. The bulk material and the corresponding thin film material with the same composition may exhibit different mechanical properties and microstructure evolution behavior after annealing. So, this paper will comparatively study the effect of annealing treatment on the microstructure of the supersaturated copper alloy film and bulks.

In the paper, Cu-Zr alloy films with different thickness were prepared on the Polyimide (PI) substrates by magnetron sputtering. Cu-Cr bulk alloys were prepared by vacuum melting technique. Some of the samples were vacuum annealed. XRD, FESEM, EDS, and metallographic microscopy were used to characterize the phase, surface morphology, composition of the alloy film and bulk alloy before and after annealing. The effects of annealing treatment on the surface morphology and phase of the alloy film and block were investigated.

The Results show that Cr content has an important influence on the surface morphology and microstructure of the alloy film. The addition of proper amount of Cr can inhibit the growth of Cu crystal grains. When the Cr content is low, the Cu (111) diffraction peak can be observed in the XRD pattern of the alloy film, and not Cr diffraction peak. However, both Cu and Cr diffraction peak can be observed in the XRD pattern of the alloy bulk material, which is different from the alloy film. The microstructure of bulk Cu-Cr alloy and the film exhibit different evolution behaviors after annealing. There are a large amount of Cr dendrites precipitated on the surface of the bulk after annealing. It is interesting to point out that a large number of polyhedral pure Cu particles formed spontaneously on the surface of Cu-Zr alloy films which is obviously different from the bulk Cu-Cr alloy, and the particle formation mechanism was analyzed.

Keywords: Cu-Cr film, Cu-Cr alloy bluk, annealing, microstructure

High temperature oxidation behaviors of HVOF-sprayed

Cr₂C₃-NiCr coating in air at 800 °C

Zupeng Yan^{1,2}, Xiangjun Chen^{1,2}, Kai Hu^{1,2}, Yonghong Wen^{1,2}, Xia Liu^{1,2}, Shihong Zhang^{1,2}

(1. Research Center of Modern Surface & Interface Engineering, AHUT, China;

2. School of Materials Science and Engineering, AHUT, Maanshan 243002, China)

Abstract: Cr₂C₃-NiCr coating was prepared by high velocity oxygen fuel spraying technology and its high temperature oxidation resistance was studied at 800 °C. X-ray diffractometry, Raman spectroscopy, and scanning electron microscopy were utilized to analyze the microstructure and phase composition of the coatings before and after oxidation. The mechanical properties of the coating were characterized by HV-1000 Vickers hardness tester. Results showed that the coating possessed a dense structure and a low porosity. What's more, the coating showed excellent oxidation resistance, which is attributed to the formation of the oxide film with Cr₂O₃ as the main component on the surface. However, owing to the decomposition of a small amount of Cr₂C₃ ceramic phase, the hardness of the coating after oxidation had a certain degree of decline.

Keywords: high velocity oxygen fuel spraying, Cr₂C₃-NiCr, microstructure, high temperature oxidation

Grain morphology evolution and texture characterization of wire and

arc additive manufactured Ti-6Al-4V

Jian Wang^{1,2}, Fenggang Liu^{1,2}

(1. State Key Laboratory of Solidification Processing, Northwestern Polytechnical University, China;

2. Key Laboratory of Metal High Performance Additive Manufacturing and Innovative Design, MIIT China, Northwestern Polytechnical University, China)

Abstract: In this study, four straight walls of Ti-6Al-4V titanium alloy were fabricated by Wire and arc additive manufacturing (WAAM) to investigate the effect of deposition parameters on grain morphology evolution and texture characterization in the building direction. A certain volume fraction of equiaxed β grain appeared at the bottom of the wall and can be controlled by deposition parameters, while the columnar β grain zone was on the equiaxed β grain zone. It is indicated that the formation of equiaxed β grains at the bottom of the wall initiated from the recrystallization. There were the large residual stress, strain, and high heating rate when depositing the first several layers near the substrate, which can induce the recrystallization of the already-deposited layers at the bottom of the wall. However, the preferred crystallographic orientations along the building direction formed gradually during the deposition process, then the β grains began to grow epitaxially from the already-deposited layers, and changed to columnar β grains, which lead to a strong $\langle 001 \rangle$ fiber texture in the building direction. In addition, there are also some equiaxed β grains at the top surface of the wall due to the occurrence of the columnar to equiaxed grain transition (CET) in the molten pool.

Keywords: wire and arc additive manufacturing, Ti-6Al-4V alloy, grain morphology, texture characterization

The thermal fatigue behavior and cracking characteristics of ductile Ni-resist cast iron for exhaust manifolds

Yunlong Yang

(Jilin Vocational College of Industry and Technology, Jilin, China)

yy11976@126.com

Abstract: Ductile Ni-resist cast iron (DNCI) with nickel content about 28% was exploited by Jilin University and First Automotive Works (FAW) together. It was used for exhaust manifolds instead of the high Si-Mo nodular cast iron. This study investigates the thermal fatigue cracking behavior of the DNCI. The repeated heating/cooling tests are performed under cyclic heating at various temperatures. Experimental results indicate that the thermal fatigue cracking resistance decreases with the increase of the T_{max} . The shortest period for crack initiation was individually 18-24 times and 34-42 times and 40-55 times associated with heating temperature, when the holding time was about 10 min at T_{max} , and after quenching with tap-water. The major sources of cracks propagation were generally at the eutectic oxide boundary region and the region of the austenitic phase boundary by mean of SEM/EDX. According to thermal fatigue test results and analysis, it is thought that the reasonable working temperature of the DNCI is not more than 950 °C.

Keywords: ductile Ni-resist cast iron, thermal fatigue crack, exhaust manifold

Influence of Al content on microstructure and properties of TC4 alloys fabricated by laser additive manufacturing

Guiwei Zhang, Cunshan Wang

(Dalian University of Technology)

laser@dlut.edu.cn

Abstract: In the present work, TC4 alloys with different Al additions were produced by laser additive manufacturing on the TC4 substrate. The influences of Al content on microstructure and properties of the alloys were investigated in detail. The results showed that these alloys are composed of the β -Ti and the α -Ti solid solutions. With the increase of Al addition, the volume fraction of the β -Ti solid solution decreases, while that of α -Ti solid solution increases, leading to improved corrosion resistance, enhanced mechanical and tribological properties. Meanwhile, the formability of the alloys is significantly increased due to the decrease in the solidification temperature range.

Keywords: laser additive manufacturing, TC4 alloy, microstructure, property

Microstructure and electrochemical anodic behavior of Inconel 718 fabricated by high-power laser solid forming

Pengfei Guo^{1,2}, Xin Lin^{1,2}, Yongming Ren^{1,2}, Jianjun Xu^{1,2}, Jiaqiang Li^{1,2}, Yufeng Zhang^{1,2},
Jing Chen^{1,2}, Weidong Huang^{1,2}

- (1. State Key Laboratory of Solidification Processing, Northwestern Polytechnical University, China;
2. Key Laboratory of Metal High Performance Additive Manufacturing and Innovative Design, MIIT
China, Northwestern Polytechnical University, China)

xlin@nwpu.edu.cn

Abstract: The surface quality of the high-power laser solid forming (LSF)-fabricated superalloys, titanium alloys or other difficult processing materials is inferior to the traditional machining surface, which has severely limited the wide application of this technology. Here, we have systematically investigated the surface improvement of the high-power LSF-produced Inconel 718 by electrochemical method. The central issues consist of forming features (including surface microstructure characteristics and surface morphology) and the corresponding electrochemical anodic behavior (including electrochemical dissolution behavior and surface levelling mechanism). The electrochemical results show that, the surface energy distinction between the horizontal section and vertical section leads to no difference of the transpassive current density in 10wt% NaNO₃ solution up to 2.5 V owing to the existence of the passive film. The micro-morphologies analysis indicates that the high current density leads to a smooth micro-morphology due to the higher detachment rate of the interdendritic phases, as well as the surface products. The numerical simulations suggest that the surface peak dissolved faster than the depressions during the electrochemical levelling process due to the higher local current density on the surface peak. Importantly, a detailed microstructure selection map for as-deposited Inconel 718, current density-potential map during anodic dissolution process and electrochemical levelling mechanism of its wavy surfaces were developed and proposed, respectively. This work is capable of bridging links between LSF-process conditions, forming features and electrochemical anodic behavior. Further, this investigation provides an insight to solve the difficulty on manufacturing of the large high performance metallic components with high efficiency, high precision and low cost.

Keywords: laser solid forming, Inconel 718, electrochemical anodic behaviour, passive film, electrochemical levelling

A constitutive model for high temperature deformation of AZ31 magnesium alloy

Mengling Wu^{1,2}, Xin Wang^{1,2}, Jing Chen^{1,2}, Qi Wang^{1,2}, Yanwen Wu^{1,2}

- (1. Jiangsu Key Laboratory of Advanced Structural Materials and Application Technology, China;
2. School of Materials Science and Engineering, Nanjing Institute of Technology, China)

wmlzl@njit.edu.cn

Abstract: High temperature deformation behavior of AZ31 magnesium alloy is investigated by tensile test in the temperature between 190 °C and 250 °C and strain rates in a wide range from $5 \times 10^{-4} \text{ s}^{-1}$ to $5 \times 10^{-3} \text{ s}^{-1}$. Base on the stress-strain relationship, a constitutive model for high temperature deformation of AZ31 magnesium alloy is developed. The deformation activation energy of ultra-fine grained AZ31 magnesium alloy under this test condition is 118.37 kJ/mol.

Keywords: AZ31 magnesium alloy, high temperature deformation, constitutive model

Microstructure and wear resistance of in-situ synthesized (Ti₃Al+TiB)/Ti composites by laser surface additive manufacturing

Yueqiao Feng, Zhuguo Li
(Shanghai Jiao Tong University)
lizg@sjtu.edu.cn

Abstract: Titanium alloys are widely used in almost every domain of industry, but low hardness and poor tribological properties restrict the application of titanium alloys under severe wear and friction conditions. Laser surface additive manufacturing (LSAM) is an advanced direct metal deposition technique and has many advantages over conventional manufacturing processes. Therefore in this study, a new laser additive manufacturing materials system of pure Ti and AlB₂ mixed powder was designed to fabricate a new type of in-situ synthesized (Ti₃Al+TiB)/Ti composite coating on titanium alloys (Ti6Al4V) to improve the wear resistance of the substrate effectively.

Keywords: titanium alloy, laser additive manufacturing, microstructure, wear resistance

Localized grain boundary melting induced HAZ liquation cracking during laser solid forming of IN-738LC superalloy

Jianjun Xu^{1,2}, Xin Lin^{1,2}, Pengfei Guo^{1,2}, Haiou Yang^{1,2}, Lei Xue³, Weidong Huang^{1,2}
(1. State Key Laboratory of Solidification Processing, Northwestern Polytechnical University, China;
2. Key Laboratory of Metal High Performance Additive Manufacturing and Innovative Design, MIIT
China, Northwestern Polytechnical University, China;
3. Xi'an Bright Laser Technologies LTD, Xiyuan, Northwestern Polytechnical University, China)
xlin@nwpu.edu.cn

Abstract: The HAZ liquation cracking mechanism of laser solid formed IN-738LC superalloy during laser remelting was investigated. Microstructural analysis of the heat-affected zone revealed that the cracks are mainly distributed along the grain boundary and mainly caused by the localized melting of semicontinuous γ - γ' eutectic. The solute segregation behavior of IN-738LC alloy in laser solid forming was analyzed by GK model and Scheil model. It is found that the significant enrichment in residual liquid of γ - γ' eutectic forming elements at the final stage of solidification (solid fraction, $f_s \approx 0.87$) in the molten pool is the main cause of the formation of semicontinuous γ - γ' eutectic at grain boundary in the deposit. The solid dissolution of γ' phases in HAZ decreased away from remelting zone, and the γ' phases are completely dissolved in the grain after the localized melting of γ - γ' eutectic occur at the grain boundary.

Keywords: laser solid forming, IN-738LC, liquation cracking, microsegregation

The effect of micro-B addition on microstructure and mechanical properties of laser additive manufacturing Ti-6Al-4V

Aitang Xue, Xin Lin, Weidong Huang

(State Key Laboratory of Solidification Processing, Northwestern Polytechnical University, Xi'an, China)

Abstract: The Laser solid forming titanium alloy parts are different from casting alloys and wrought alloys in microstructure characteristics, phase constitution and performance.

Thus, the composition of existing materials may fails to give full play to its strong features during LSF. Based on the characteristics of LSF, in order to further improve the comprehensive mechanical properties of LSF titanium alloy parts, this paper chose the most widely used Ti-6Al-4V and titanium alloy refinement element B, combined with the thermodynamics calculation, studied the phases and microstructure of LSF Ti-6Al-4V-xB and analyzed the effect of B on them. This is an important prerequisite to improve the performance of LSF titanium alloys and the primary task to develop special alloy powder. After adding trace B, the microstructure still exhibits epitaxial growth columnar crystal. Trace amounts of B reduces the size of widmanstatten α cluster and the length of α lath, but the width of which slightly increases. Moreover, grain boundary α lath becomes discontinuous. With the increase of B, the size of widmanstatten α cluster and the length of α lath further reduces, some α lath get shorter and even disappear. The morphology of TiB is equiaxial, fine acicular, plate-like and hollow hexagonal, what's more, many of them exhibit fine acicular.

Key words: titanium alloy, laser solid forming, alloying, microstructure

Mechanical properties and microstructural characterization of bronze fabricated by selective laser melting

Nie Zhen, Qingmao Zhang, Liang Guo

(South China Normal University)

zhangqm@scnu.edu.cn

Abstract: Fabricated by SLM, copper alloy, as a new material, have arouse interest in aerospace engineering, automobile, jewelry and medical fields. Specimens have been manufactured via SLM of bronze powder and been heat treated at 673, 873 and 1073 K(400, 600, and 800 °C) for 120 min. Room-temperature tensile tests and microstructure characterization selected samples in different heat-treated conditions. Tensile tests have shown that heat treatment results in lower yield strength with increases in ductility, under the condition of recrystallization and eliminating micro segregation. This experiment has demonstrated that metal ductility of sample fabricated by SLM was higher than casting material ,and it was related to high cooling rate imposed by laser processing.

Keywords: selective laser melting, heat treatment, bronze